

Supporting Information

Investigating the Competing E2 and S_N2 Mechanisms for the Microsolvated HO⁻(H₂O)_{n=0-4} + CH₃CH₂X (X = Cl, Br, I) reactions

Xiangyu Wu, Shaowen Zhang,* Jing Xie*

Key Laboratory of Cluster Science of Ministry of Education, School of Chemistry and Chemical Engineering, Beijing Institute of Technology, Beijing 100081, China

Corresponding author:

Shaowen Zhang, swzhang@bit.edu.cn

Jing Xie, jingxie@bit.edu.cn

Table of Contents

Table of Contents	S2
Table S1 Selected previous researches on $X^- + CH_3CH_2Y$ type reactions	S4
Table S2 Structural isomers along the PESs of $HO^-(H_2O)_n + CH_3CH_2X$ ($X = Cl, Br, I$) S_N2 and E2 reactions optimized at MP2/ECP/d level.	S5
Table S3 Comparison of reaction enthalpies (kcal/mol) for $HO^- + CH_3CH_2X$ ($X = Cl, Br, I$) using ECP/t basis set and different methods.	S6
Table S4 Experimental standard molar enthalpy of formation of individual substances from different database.	S7
Table S5 Relative energies (kcal/mol) of the transition states of $HO^- + CH_3CH_2I$ reaction at different levels of theory with ECP/d basis set	S8
Table S6 Reaction energies (in kcal/mol) of the S_N2 and E2 product channels of $HO^-(H_2O)_{n=0,1,2} + CH_3CH_2X$ ($X = Cl, Br, I$) reactions calculated at CCSD(T)/PP/t//MP2/ECP/d level of theory.	S9
Table S7 Selected bond distances (Å) of inv- S_N2 -TS and anti-E2-TS structures for $HO^-(H_2O)_n + CH_3CH_2X$ ($X = Cl, Br, I$) reactions as optimized by MP2/ECP/d method.	S10
Table S8 Harmonic frequencies (cm ⁻¹) of the transition states of $HO^- + CH_3CH_2I$ at the level of MP2/ECP/d.	S11
Table S9 Overall barrier of inv- S_N2 and anti-E2 transition states as calculated with MP2/ECP/d and PCM(water)-MP2/ECP/d method.	S12
Table S10 Overall barrier of inv- S_N2 and anti-E2 transition states as calculated with CCSD(T)/PPt//MP2/ECP/d and PCM(water)-CCSD(T)/PP/t//MP2/ECP/d method.	S13
Table S11 Calculated proton affinity and ethyl cation affinity of nucleophile $HO^-(H_2O)_n$	S14
Table S12 Energy (in eV) of the HOMO orbitals of the $HO^-(H_2O)_n$ using different methods.	S14
Table S13 Looseness (%L) and asymmetry index (%AS) of the inv- S_N2 transition structures.	S15
Table S14 Looseness (%L) and asymmetry index (%AS) of the anti-E2 transition structures.	S16
Table S15 NPA charge distributions for the inv- S_N2 -TS. ($X = Cl, Br, I$)	S17
Table S16 NPA charge distributions for the anti-E2-TS. ($X = Cl, Br, I$)	S18
Table S17 Energy decomposition analysis of inv- S_N2 and anti-E2 transition structure at MP2/ECP/d level.	S19
Table S18 Selected bond distances (Å) of inv- S_N2 -TS and anti-E2-TS structures for $HO^-(H_2O)_{n=0-4} + CH_3CH_2X$ ($X = Cl, Br, I$) reactions as optimized by PCM(water)-MP2/ECP/d method.	S20

Table S19	Calculated overall barrier of inv-S _N 2 and anti-E2 transition states using different models. MP2/ECP/d method was used.	S21
Table S20	Energy differences between gas-phase and PCM calculations and the compositions.	S23
Table S21	Barrier differences between gas-phase and PCM calculations and the compositions.	S24
Figure S1	IRC calculation of the anti-E2-TS/inv-S _N 2-TS of HO ⁻ + CH ₃ CH ₂ I S _N 2 reaction	S25
Figure S2	Mechanic spectra of the competing bimolecular nucleophilic substitution (S _N 2) reaction vs. bimolecular elimination (E2) reaction	S26
Figure S3	Structure comparison of anti-E2-TS and inv-S _N 2-TS optimized by CAM-B3LYP, M06-2X, M06, and MP2 method	S27
Figure S4	Potential Energy Profiles of HO ⁻ (H ₂ O) _{n=0,1,2} + CH ₃ CH ₂ I	S28
Figure S5	Potential Energy Profiles of HO ⁻ (H ₂ O) _{n=0,1,2} + CH ₃ CH ₂ Br	S29
Figure S6	Potential Energy Profiles of HO ⁻ (H ₂ O) _{n=0,1,2} + CH ₃ CH ₂ Cl	S30
Figure S7	IBOs of HO ⁻ + CH ₃ CH ₂ Cl	S31
Figure S8	IBOs of HO ⁻ (H ₂ O) + CH ₃ CH ₂ Cl	S32
Figure S9	IBOs of HO ⁻ (H ₂ O) ₂ + CH ₃ CH ₂ Cl	S33
Figure S10	Mirror images of the pre-reaction complexes of HO ⁻ (H ₂ O) + CH ₂ CH ₃ Y reactions.	S34
Figure S11	Plots of barrier heights vs geometric looseness (%L [‡]) and asymmetry index(%AS [‡])	S35
Figure S12	Plots of inv-S _N 2 and anti-S _N 2 barrier heights vs asymmetry of charge distribution Δq(X–O)	S36
Figure S13	Energy decomposition analysis of inv-S _N 2 and anti-E2 transition structure between HO ⁻ (H ₂ O) _n and CH ₃ CH ₂ Cl/CH ₃ CH ₂ Br.	S37
Figure S14	Potential Energy Profiles of HO ⁻ + CH ₃ CH ₂ X using PCM model	S38
Figure S15	Comparison of barrier heights of a) inv-S _N 2 and b) anti-E2 transition states and c) barrier difference ΔΔE [‡] between gas-phase, PCM, and PCM-SP methods.	S39
References		S40

Table S1 Selected previous researches on $X^- + CH_3CH_2Y$ type reactions.

Nucleophile, X^-	Leaving group, Y	Reference
F^-, Cl^-	F, Cl	¹ Minato, <i>J. Am. Chem. Soc.</i> 1988 , <i>110</i> (14), 4586
$F^-, PH^- 2$	Cl	² Gronert, <i>J. Am. Chem. Soc.</i> 1991 , <i>113</i> (16), 6041
F^-	F	³ Bickelhaupt, <i>J. Am. Chem. Soc.</i> 1993 , <i>115</i> (20), 9160
F^-	F	⁴ Merrill, <i>J. Phys. Chem. A</i> 1997 , <i>101</i> (2), 208
F^-	Cl	⁵ Mugnai, <i>J. Phys. Chem. A</i> 2003 , <i>107</i> (14), 2540
F^-, Cl^-	F, Cl	⁶ Bento, <i>J. Chem. Theory Comput.</i> 2008 , <i>6</i> (4), 929
F^-, Cl^-	F, Cl	⁷ Zhao, <i>J. Chem. Theory Comput.</i> 2010 , <i>6</i> (4), 1104
F^-, Cl^-	F, Cl	⁸ Swart, <i>J. Chem. Theory Comput.</i> 2010 , <i>6</i> (10), 3145
F^-	I	⁹ Yang, <i>J. Phys. Chem. A</i> 2017 , <i>121</i> (5), 1078
F^-	Cl	¹⁰ Tajti, <i>J. Phys. Chem. A</i> 2017 , <i>121</i> (14), 2847
F^-	I	¹¹ Carrascosa, <i>Nat. Commun.</i> 2017 , <i>8</i> (1), 25
F^-	Br	¹² Satpathy, <i>J. Phys. Chem. A</i> 2018 , <i>122</i> (27), 5861

Note: Zhao *et al.*¹³ have analyzed the performance of various density functionals and found that M06 and M06-2X performed better. Satpathy *et al.*¹² have tested several functionals for the reaction of $F^- + CH_3CH_3Br$ and found that M06 is the most reliable density functional according to the mean absolute error. Yang *et al.*⁹ have studied the S_N2 and E2 competing reactions of $F^- + CH_3CH_2I$ and found that MP2 has the best accuracy and the consistency of CAM-B3LYP and M06 with the benchmark is better than other density functional. B97-1 has been used many times in the study of $OH^- + CH_3I$ reaction,¹⁴⁻¹⁶ which has been confirmed to be in good agreement with the experiment. Previous studies^{17, 18} have shown that the potential energy surfaces (PES) for S_N2 reactions obtained by OLYP and B3LYP are both compare well with the *ab initio* benchmark PES. Therefore, we did a series of calculations using M06, M06-2X, B3LYP, B97-1, CAM-B3LYP, OLYP and MP2 with several basis sets, and the results are shown in Table S2-S3.

Table S2. Structural isomers along the PESs of $\text{HO}^-(\text{H}_2\text{O})_n + \text{CH}_3\text{CH}_2\text{X}$ ($\text{X} = \text{Cl}, \text{Br}, \text{I}$) $\text{S}_{\text{N}}2$ and $\text{E}2$ reactions optimized at MP2/ECP/d level. MP2 electronic energies in relative to $\text{HO}^-(\text{H}_2\text{O})_n + \text{CH}_3\text{CH}_2\text{X}$ are reported.

MP2/ECP/d	X = I					X = Br					X = Cl				
Without ZPE	n=0	n=1	n=2	n=3	n=4	n=0	n=1	n=2	n=3	n=4	n=0	n=1	n=2	n=3	n=4
$\text{HO}^-(\text{H}_2\text{O})_n + \text{CH}_3\text{CH}_2\text{X}$	0.0	0.0	0.0	0.0	0.0	0.0	0.0	0.0	0.0	0.0	0.0	0.0	0.0	0.0	0.0
$[\text{HO}^-(\text{H}_2\text{O})_n + \text{CH}_3\text{CH}_2\text{X}] \cdot 2$	/	/	/	1.1	0.6	/	/	/	1.1	0.6	/	/	/	1.1	0.6
aRC	-19.9	-17.4	-15.5	/	/	-19.5	-17.0	-15.1	/	/	-18.7	-16.3	-14.5	/	/
bRC	-19.5	-17.4	-15.9	/	/	-19.5	-17.0	-15.5	/	/	-18.7	-16.3	-14.5	/	/
cRC	-19.9	-17.4	-16.1	/	/	-19.5	-17.0	-15.7	/	/	-18.7	-16.3	-14.9	/	/
dRC	-19.9	-17.4	-15.9	/	/	-19.5	-17.0	-15.6	/	/	-18.7	-16.3	-14.8	/	/
aTS (inv- $\text{S}_{\text{N}}2$)	-17.8	-10.9	-5.9	-0.3	5.3	-15.8	-9.0	-3.9	1.7	6.9	-13.1	-6.2	-1.0	4.7	9.9
aTS-2	/	/	-3.7	0.3	5.3	/	/	-2.1	1.8	7.3	/	/	0.8	4.9	10.3
aTS-3	/	/	/	0.8	/	/	/	/	2.8	/	/	/	/	5.9	/
aTS-4	/	/	/	/	/	/	/	/	6.1	/	/	/	/	8.5	/
bTS (ret- $\text{S}_{\text{N}}2$)	14.3	20.9	30.5	/	/	18.3	24.2	33.1	/	/	22.4	28.3	37.0	/	/
cTS (anti-E2)	-16.7	-8.7	-2.0	5.0	8.5	-15.2	-6.7	0.4	7.4	10.8	-13.2	-4.2	3.2	10.4	14.0
cTS-2	/	/	-1.3	5.5	9.5	/	/	1.1	8.1	11.6	/	/	3.8	11.3	14.6
cTS-3	/	/	5.2	9.0	10.2	/	/	6.4	10.2	12.2	/	/	8.6	12.5	18.0
cTS-4	/	/	/	/	12.3	/	/	/	/	14.9	/	/	/	/	/
dTS (syn-E2)	-8.6	-1.5	4.5	/	/	-6.9	0.1	6.2	/	/	-5.3	2.5	8.8	/	/
aPC	-70.0	-63.4	-54.3	/	/	-65.5	-61.0	-36.6	/	/	-60.0	-43.6	-31.4	/	/
aPC-2	-76.9	-61.5	-50.2	/	/	-73.5	-58.7	-47.5	/	/	-69.2	-54.9	-44.0	/	/
aPC-3	/	/	/	/	/	/	-61.2	-53.0	/	/	/	-57.4	-50.3	/	/
bPC	-76.9	-63.4	-54.0	/	/	-73.5	-61.2	-52.9	/	/	-69.2	-57.6	-49.7	/	/
cPC	-65.6	-52.9	-43.5	/	/	-62.4	-50.8	-42.6	/	/	-58.0	-47.3	-39.4	/	/
dPC	-65.6	-52.9	-42.1	/	/	-62.4	-50.8	-41.4	/	/	-58.0	-47.3	-38.4	/	/
$\text{C}_2\text{H}_4 + \text{Y}^- + (\text{n}+1)\text{H}_2\text{O}$	-47.6	-20.9	1.1	/	/	-42.4	-15.7	6.3	/	/	-36.8	-10.1	11.9	/	/
$\text{CH}_3\text{CH}_2\text{OH} + \text{Y}^- + \text{nH}_2\text{O}$	-62.7	-36.0	-14.0	/	/	-57.5	-30.7	-8.7	/	/	-51.9	-25.2	-3.2	/	/

Table S3 Comparison of reaction enthalpies (kcal/mol) for $\text{HO}^- + \text{CH}_3\text{CH}_2\text{X}$ ($\text{X} = \text{Cl}, \text{Br}, \text{I}$) using ECP/t basis set and different methods.^a

	B3LYP	B97-1	OLYP	MP2	CCSD(T)^b	Exp.^c
$\text{CH}_3\text{CH}_2\text{OH} + \text{Cl}^-$	-51.8	-52.1	-48.8	-47.1	-50.0	-51.1/-50.8
$\text{CH}_2=\text{CH}_2 + \text{H}_2\text{O} + \text{Cl}^-$	-42.4	-39.7	-42.0	-35.0	-38.8	-40.2/-39.9
$\text{CH}_3\text{CH}_2\text{OH} + \text{Br}^-$	-59.5	-59.6	-55.9	-51.9	-55.2	-59.6/-58.9
$\text{CH}_2=\text{CH}_2 + \text{H}_2\text{O} + \text{Br}^-$	-50.0	-47.1	-49.1	-39.8	-44.0	-48.7/-47.9
$\text{CH}_3\text{CH}_2\text{OH} + \text{I}^-$	-65.0	-65.3	-61.2	-53.8	-61.1	-66.6/-66.5
$\text{CH}_2=\text{CH}_2 + \text{H}_2\text{O} + \text{I}^-$	-55.6	-52.8	-54.4	-41.7	-49.9	-55.7/-55.6
MAE	1.0/1.3	1.2/1.2	2.5/2.5	8.8/8.4	3.8/3.4	

^aFor MP2 and DFT methods, the basis set is ECP/t. For the CCSD(T) method, the basis set is PP/t.

^bThe values are obtained by the sum of the single point energy calculated from CCSD(T)/PP/t plus the enthalpy correction given by MP2/ECP/t method.

^cThe experimental values are enthalpies at 298.15 K in kcal/mol, which are from NIST database¹⁹ and CRC Handbook of Chemistry and Physics²⁰/Active Thermochemical Table(ATcT)²¹ respectively.

Table S4 Experimental standard molar enthalpy of formation of individual substances from different database.

		$\Delta_f H^\circ$ (kJ/mol)	
	NIST	^c CRC handbook	^d ATcT
HO ⁻	-143.6^a	/	-139.06
Cl ⁻	-234.0^a	/	-227.346
Br ⁻	-219.0^a	/	-212.685
I ⁻	-194.6^a	/	-188.396
H ₂ O	-241.8 ^b	-241.8	-241.836
CH ₂ =CH ₂	52.5 ^b	52.4	52.35
CH ₃ CH ₂ Cl	-112.1 ^b	-112.1	-111.49
CH ₃ CH ₂ Br	-61.9 ^b	-61.9	-63.33
CH ₃ CH ₂ I	-7.2 ^b	-8.1	-7.18
CH ₃ CH ₂ OH	-234.7 ^b	-234.8	-235.03

References

^aChase, M.W., Jr., NIST-JANAF Thermochemical Tables, Fourth Edition, J. Phys. Chem. Ref. Data, Monograph 9, 1998, 1-1951.

^bE. P.J. Linstrom and W.G. Mallard, NIST Chemistry WebBook, NIST Standard Reference Database Number 69, National Institute of Standards and Technology, Gaithersburg MD, 20899, <https://doi.org/10.18434/T4D303> (retrieved July 22, 2021)).

^cD. R. Lide, CRC Handbook of Chemistry and Physics, Internet Version 2005, CRC Press, Boca Raton, FL, 2005.

^dB. R. a. D. H. Bross, Active Thermochemical Tables (ATcT) values based on ver. 1.122p of the Thermochemical Network, available at ATcT.anl.gov).

Table S5 Relative energies (kcal/mol) of the transition states of HO⁻ + CH₃CH₂I reaction at different levels of theory with ECP/d basis set.

	anti-E2-TS/inv-S _N 2-TS		
	ΔE	ΔH (0 K)	ΔH (298.15 K)
B3LYP	-22.2	-19.9	-20.4
B97-1	-22.6	-20.7	-21.2
OLYP	-20.3	-17.8	-18.1
	anti-E2-TS		
	ΔE	ΔH (0 K)	ΔH (298.15 K)
CAM-B3LYP	-18.8	-19.7	-20.1
M06	-20.6	-21.6	-22.0
M06-2X	-20.5	-21.4	-21.8
MP2	-16.7	-18.7	-19.1
CCSD(T) ^a	-18.4	-20.4	-20.7
	ΔE	ΔH (0 K)	ΔH (298.15 K)
inv-S _N 2-TS			

^aThe ΔH values are obtained by the sum of the single point energy calculated from CCSD(T)/PP/t plus the zero-point correction and the thermal correction to enthalpy calculated from MP2/ECP/d.

Table S6. Reaction energies (in kcal/mol) of the S_N2 and E2 product channels of HO⁻(H₂O)_{n=0,1,2} + CH₃CH₂X (X = Cl, Br, I) reactions calculated at CCSD(T)/PP/t//MP2/ECP/d level of theory.

n		X = Cl		X = Br		X = I	
		E	H(298.15K)	E	H(298.15K)	E	H(298.15K)
0	Reactant	HO ⁻ + CH ₃ CH ₂ X	0.0	0.0	0.0	0.0	0.0
	Product (S _N 2)	CH ₃ CH ₂ OH + X ⁻	-52.9	-50.3	-58.5	-55.6	-64.8
	Product (E2)	CH ₂ =CH ₂ + H ₂ O + X ⁻	-38.7	-39.4	-44.2	-44.7	-50.5
		CH ₂ =CH ₂ (H ₂ O) + X ⁻	-42.2	-42.1	-47.8	-47.4	-54.1
		CH ₂ =CH ₂ + X ⁻ (H ₂ O)	-54.3	-54.7	-58.7	-58.7	-63.0
1	Reactant	HO ⁻ (H ₂ O) + CH ₃ CH ₂ X	0.0	0.0	0.0	0.0	0.0
		HO ⁻ + CH ₃ CH ₂ X(H ₂ O)	21.1	22.6	20.6	22.0	20.6
	Product (S _N 2)	CH ₃ CH ₂ OH + X ⁻ + H ₂ O	-25.1	-22.4	-30.7	-27.7	-37.0
		CH ₃ CH ₂ OH + X ⁻ (H ₂ O)	-40.8	-37.7	-45.1	-41.8	-49.4
		CH ₃ CH ₂ OH(H ₂ O) + X ⁻	-33.2	-28.9	-38.8	-34.1	-45.1
	Product (E2)	CH ₂ =CH ₂ + 2H ₂ O + X ⁻	-10.9	-11.5	-16.5	-16.8	-22.8
		CH ₂ =CH ₂ (H ₂ O) ₂ + X ⁻	-22.1	-19.6	-27.6	-24.9	-33.9
		CH ₂ =CH ₂ + X ⁻ (H ₂ O) ₂	-42.4	-40.9	-46.1	-44.3	-49.1
		CH ₂ =CH ₂ (H ₂ O) + X ⁻ (H ₂ O)	-30.1	-29.5	-34.4	-33.6	-38.7
2	Reactant	HO ⁻ (H ₂ O) ₂ + CH ₃ CH ₂ X	0.0	0.0	0.0	0.0	0.0
		HO ⁻ + CH ₃ CH ₂ X(H ₂ O) ₂	35.4	36.5	34.7	35.8	34.7
	Product (S _N 2)	CH ₃ CH ₂ OH + X ⁻ + 2H ₂ O	-2.5	-1.9	-8.1	-7.1	-14.4
		CH ₃ CH ₂ OH + X ⁻ (H ₂ O) ₂	-34.0	-31.3	-37.7	-34.7	-40.7
		CH ₃ CH ₂ OH(H ₂ O) ₂ + X ⁻	-21.9	-17.7	-27.5	-23.0	-33.8
		CH ₃ CH ₂ OH(H ₂ O) + X ⁻ (H ₂ O)	-26.3	-23.6	-30.6	-27.7	-34.9
	Product (E2)	CH ₂ =CH ₂ + 3H ₂ O + X ⁻	11.7	9.1	6.1	3.8	-0.2
		CH ₂ =CH ₂ (H ₂ O) ₃ + X ⁻	-8.5	-6.4	-14.1	-11.7	-20.4
		CH ₂ =CH ₂ + X ⁻ (H ₂ O) ₃	-36.8	-35.3	-40.4	-38.6	-42.7

Table S7 Selected bond distances (\AA) of inv-S_N2-TS and anti-E2-TS structures for $\text{HO}^-(\text{H}_2\text{O})_n + \text{CH}_3\text{CH}_2\text{X}$ ($\text{X} = \text{Cl}, \text{Br}, \text{I}$) reactions as optimized by MP2/ECP/d method.

inv-S _N 2-TS					anti-E2-TS				
X	n	$r(\text{O}-{}^a\text{C})$	$r({}^a\text{C}-\text{X})$	$r(\text{O}-\text{X})$	$r({}^a\text{C}-{}^\beta\text{C})$	$r(\text{O}-{}^\beta\text{H})$	$r({}^a\text{C}-\text{X})$	$r({}^\beta\text{H}-{}^\beta\text{C})$	$r({}^a\text{C}-{}^\beta\text{C})$
Cl	0	2.224	2.131	4.339	1.509	1.339	1.973	1.324	1.466
	1	2.147	2.183	4.312	1.511	1.257	2.021	1.398	1.451
	2	2.079	2.237	4.298	1.511	1.207	2.078	1.449	1.438
	3	2.070	2.247	4.297	1.512	1.191	2.085	1.468	1.435
	4	2.022	2.303	4.303	1.511	1.194	2.108	1.465	1.433
Br	0	2.268	2.245	4.495	1.509	1.393	2.120	1.284	1.467
	1	2.184	2.300	4.464	1.511	1.301	2.173	1.354	1.451
	2	2.110	2.359	4.446	1.511	1.246	2.227	1.403	1.438
	3	2.094	2.373	4.444	1.512	1.229	2.236	1.420	1.435
	4	2.042	2.431	4.448	1.511	1.226	2.265	1.427	1.431
I	0	2.318	2.411	4.707	1.511	1.452	2.313	1.247	1.472
	1	2.219	2.478	4.672	1.512	1.346	2.374	1.316	1.455
	2	2.137	2.542	4.652	1.512	1.283	2.429	1.366	1.442
	3	2.077	2.603	4.651	1.513	1.262	2.439	1.383	1.439
	4	2.060	2.625	4.655	1.512	1.250	2.473	1.400	1.433
ret-S _N 2-TS					syn-E2-TS				
X	n	$r(\text{O}-{}^a\text{C})$	$r({}^a\text{C}-\text{X})$	$r(\text{O}-\text{X})$	$r({}^a\text{C}-{}^\beta\text{C})$	$r(\text{O}-{}^\beta\text{H})$	$r({}^a\text{C}-\text{X})$	$r({}^\beta\text{H}-{}^\beta\text{C})$	$r({}^a\text{C}-{}^\beta\text{C})$
Cl	0	2.153	2.251	2.908	1.507	1.256	1.906	1.387	1.491
	1	2.149	2.311	2.902	1.502	1.255	1.979	1.381	1.470
	2	2.148	2.294	2.891	1.504	1.252	2.036	1.379	1.456
Br	0	2.176	2.384	3.026	1.507	1.305	2.072	1.338	1.486
	1	2.166	2.445	3.017	1.503	1.303	2.145	1.333	1.466
	2	2.165	2.433	3.009	1.505	1.291	2.199	1.336	1.454
I	0	2.197	2.565	3.176	1.509	1.348	2.291	1.300	1.482
	1	2.175	2.631	3.170	1.505	1.333	2.366	1.306	1.463
	2	2.175	2.631	3.170	1.507	1.314	2.418	1.315	1.452

Table S8. Harmonic frequencies (cm^{-1}) of the transition states of $\text{HO}^- + \text{CH}_3\text{CH}_2\text{I}$ at the level of MP2/ECP/d.

inv-S _N 2-TS	ret-S _N 2-TS	anti-E2-TS	syn-E2-TS
-380	-603	-571	-993
158	110	26	73
170	157	71	93
211	178	75	218
211	260	195	265
249	332	374	421
308	404	501	441
497	615	503	536
776	738	734	675
912	851	928	772
955	983	974	885
1021	1076	1000	1011
1093	1150	1174	1085
1216	1227	1229	1178
1347	1361	1257	1231
1448	1440	1426	1407
1471	1467	1447	1433
1479	1479	1480	1472
3053	2985	1512	1576
3151	3074	3077	3042
3155	3117	3134	3094
3251	3190	3145	3122
3368	3216	3216	3171
3770	3783	3797	3795

Table S9 Overall barrier of inv-S_N2 and anti-E2 transition states as calculated with MP2/ECP/d and PCM(water)-MP2/ECP/d method. *E* is electronic energy and *H* is enthalpy at 298.15 K.

kcal/mol	inv-S _N 2						anti-E2						^a $\Delta\Delta E^\ddagger$			^b $\Delta\Delta H^\ddagger$				
	X		Cl		Br		I		Cl		Br		I		Cl	Br	I	Cl	Br	I
			ΔE^\ddagger	ΔH^\ddagger	ΔE^\ddagger	ΔH^\ddagger	ΔE^\ddagger	ΔH^\ddagger	ΔE^\ddagger	ΔH^\ddagger										
0	-13.1	-12.9	-15.8	-15.6	-17.8	-17.5	-13.2	-16.3	-15.2	-18.0	-16.7	-19.1	-0.1	0.6	1.1	-3.3	-2.4	-1.5		
1	-6.2	-4.4	-9.0	-7.1	-10.9	-9.0	-4.2	-5.7	-6.7	-8.0	-8.7	-9.8	2.0	2.3	2.2	-1.3	-0.9	-0.8		
2	-1.0	0.8	-3.9	-2.0	-5.9	-3.9	3.2	1.6	0.4	-1.1	-2.0	-3.3	4.2	4.3	3.9	0.7	0.9	0.6		
3	4.7	5.9	1.7	3.0	-0.3	1.5	10.4	8.5	7.4	5.7	5.0	3.4	5.7	5.7	5.3	2.6	2.6	1.9		
4	9.9	10.5	6.9	7.5	5.3	6.1	14.0	11.6	10.8	8.5	8.5	6.3	4.0	3.9	3.2	1.0	1.0	0.2		
0(PCM)	11.5	11.7	10.1	10.4	9.8	10.3	13.4	10.3	12.1	9.1	11.5	8.6	1.9	2.0	1.6	-1.4	-1.4	-1.7		
1(PCM)	11.8	12.9	10.4	11.5	10.1	11.5	16.3	14.2	14.7	12.7	13.9	12.1	4.5	4.3	3.8	1.2	1.2	0.5		
2(PCM)	12.4	13.7	10.9	12.3	10.6	12.2	19.1	17.0	17.2	15.4	16.3	14.6	6.7	6.4	5.7	3.4	3.1	2.4		
3(PCM)	13.8	15.3	12.0	13.6	12.1	13.7	20.1	18.3	18.1	16.5	17.1	15.7	6.2	6.0	5.0	3.0	2.9	2.0		
4(PCM)	14.2	15.5	12.3	13.7	12.4	13.9	22.0	20.0	18.5	16.6	17.6	15.8	7.8	6.1	5.3	4.5	2.9	1.9		

$$^a\Delta\Delta E^\ddagger = \Delta E^\ddagger(\text{anti-E2}) - \Delta E^\ddagger(\text{inv-S}_N\text{2})$$

$$^b\Delta\Delta H^\ddagger = \Delta H^\ddagger(\text{anti-E2}) - \Delta H^\ddagger(\text{inv-S}_N\text{2})$$

Table S10 Overall barrier of inv-S_N2 and anti-E2 transition states as calculated with CCSD(T)/PP/t//MP2/ECP/d and PCM(water)-CCSD(T)/PP/t//MP2/ECP/d method. *E* is electronic energy and *H* is enthalpy at 298.15 K.

kcal/mol	inv-S _N 2						anti-E2						^a $\Delta\Delta E^\ddagger$			^b $\Delta\Delta H^\ddagger$			
	X	Cl		Br		I		Cl		Br		I		Cl	Br	I	Cl	Br	I
		ΔE^\ddagger	ΔH^\ddagger																
0	-15.5	-15.3	-18.5	-18.3	-20.7	-20.4	-14.6	-17.7	-16.7	-19.5	-18.4	-20.7	0.9	1.8	2.3	-2.4	-1.2	-0.3	
1	-7.7	-5.9	-10.9	-9.1	-13.1	-11.2	-4.9	-6.4	-7.5	-8.8	-9.6	-10.7	2.8	3.4	3.5	-0.5	0.3	0.5	
2	-2.3	-0.5	-5.7	-3.8	-7.9	-5.9	2.7	1.0	-0.2	-1.8	-2.6	-3.9	5.0	5.5	5.3	1.5	2.0	2.0	
0(PCM)	11.1	11.4	9.4	9.8	9.1	9.6	14.0	10.9	12.7	9.7	12.1	9.2	2.9	3.3	3	-0.5	-0.1	-0.4	
1(PCM)	12.3	13.4	10.4	11.6	10.1	11.5	17.6	15.5	15.9	13.9	15.2	13.4	5.3	5.5	5.1	2.1	2.3	1.9	
2(PCM)	13.4	14.6	11.4	12.8	11.0	12.6	21.0	18.9	19.0	17.1	18.2	16.4	7.6	7.6	7.2	4.3	4.3	3.8	

$$^a\Delta\Delta E^\ddagger = \Delta E^\ddagger(\text{anti-E2}) - \Delta E^\ddagger(\text{inv-S}_N\text{2})$$

$$^b\Delta\Delta H^\ddagger = \Delta H^\ddagger(\text{anti-E2}) - \Delta H^\ddagger(\text{inv-S}_N\text{2})$$

Table S11. Calculated proton affinity and ethyl cation affinity of nucleophile $\text{HO}^-(\text{H}_2\text{O})_n$.

n	Nucleophile	^a Proton Affinity (kcal/mol)	^b Ethyl Cation Affinity (kcal/mol)
0	HO^-	390.0	239.7
1	$\text{HO}^-(\text{H}_2\text{O})$	367.4	218.1
2	$\text{HO}^-(\text{H}_2\text{O})_2$	357.0	203.3
3	$\text{HO}^-(\text{H}_2\text{O})_3$	349.3	186.7
4	$\text{HO}^-(\text{H}_2\text{O})_4$	341.2	183.6

^aProton affinities are calculated as the reaction energy of $\text{NuH} \rightarrow \text{Nu}^- + \text{H}^+$ reaction with G3(MP2) method.²² The experimental proton affinity for HO^- is 390.3 kcal/mol (from NIST Chemistry WebBook²³), our calculated value (390.0 kcal/mol) is close to the experimental value.

^bEthyl cation affinities are calculated as the enthalpy of $\text{CH}_3\text{CH}_2\text{Nu} \rightarrow \text{Nu}^- + \text{CH}_3\text{CH}_2^+$ reaction with G3(MP2) method.

Table S12. Energy (in eV) of the HOMO orbitals of the $\text{HO}^-(\text{H}_2\text{O})_n$ using different methods.

n		MP2/ECP/d	B3LYP/ECP/ d	MP2/ECP/d(PCM)
0	HO^-	-2.95	1.05	-9.73
1	$\text{HO}^-(\text{H}_2\text{O})$	-4.60	-0.61	-10.25
2	$\text{HO}^-(\text{H}_2\text{O})_2$	-5.67	-1.52	-10.67
3	$\text{HO}^-(\text{H}_2\text{O})_3$	-6.55	-2.47	-11.07
4	$\text{HO}^-(\text{H}_2\text{O})_4$	-7.17	-3.06	-11.39

Table S13. Looseness (%L) and asymmetry index (%AS) of the inv-S_N2 transition structures.

n	inv-S _N 2 transition structure	% ^a CO [‡] _{SN2}	% ^a CX [‡] _{SN2}	%L [‡] _{SN2}	%AS [‡] _{SN2}
0	HO ⁻ ···CH ₃ CH ₂ ···Cl	54.45	17.73	72.18	36.72
1	HO ⁻ (H ₂ O)···CH ₃ CH ₂ ···Cl	49.12	20.59	69.71	28.53
2	HO ⁻ (H ₂ O) ₂ ···CH ₃ CH ₂ ···Cl	44.45	23.60	68.05	20.85
3	HO ⁻ (H ₂ O) ₃ ···CH ₃ CH ₂ ···Cl	43.81	24.12	67.93	19.69
4	HO ⁻ (H ₂ O) ₄ ···CH ₃ CH ₂ ···Cl	40.46	27.23	67.69	13.23
0	HO ⁻ ···CH ₃ CH ₂ ···Br	57.58	14.52	72.1	43.06
1	HO ⁻ (H ₂ O)···CH ₃ CH ₂ ···Br	51.69	17.37	69.06	34.32
2	HO ⁻ (H ₂ O) ₂ ···CH ₃ CH ₂ ···Br	46.56	20.35	66.91	26.21
3	HO ⁻ (H ₂ O) ₃ ···CH ₃ CH ₂ ···Br	45.44	21.06	66.51	24.38
4	HO ⁻ (H ₂ O) ₄ ···CH ₃ CH ₂ ···Br	41.86	24.04	65.91	17.82
0	HO ⁻ ···CH ₃ CH ₂ ···I	61.04	11.64	72.67	49.4
1	HO ⁻ (H ₂ O)···CH ₃ CH ₂ ···I	54.17	14.74	68.91	39.43
2	HO ⁻ (H ₂ O) ₂ ···CH ₃ CH ₂ ···I	48.48	17.70	66.18	30.78
3	HO ⁻ (H ₂ O) ₃ ···CH ₃ CH ₂ ···I	44.24	20.52	64.76	23.72
4	HO ⁻ (H ₂ O) ₄ ···CH ₃ CH ₂ ···I	43.12	21.56	64.67	21.56

Table S14. Looseness (%L) and asymmetry index (%AS) of the anti-E2 transition structures.

n	Species	% ^a CX [‡] _{E2}	% ^β HO [‡] _{E2}	% ^β C ^β H [‡] _{E2}	%CC [‡] _{E2}	%L [‡] _{E2}	%AS [‡] _{E2}	%L [‡] _{E2(2)}	%AS [‡] _{E2(2)}	%L [‡] _{E2(3)}	%AS [‡] _{E2(3)}
0	HO ⁻ ···HCH ₂ CH ₂ ···Cl	9.00	38.60	20.12	8.62	47.60	29.60	58.72	18.48	76.34	18.10
1	HO ⁻ (H ₂ O)···HCH ₂ CH ₂ ···Cl	11.69	30.10	26.77	7.56	41.79	18.41	56.87	3.33	76.12	-0.80
2	HO ⁻ (H ₂ O) ₂ ···HCH ₂ CH ₂ ···Cl	14.80	24.96	31.39	6.57	39.76	10.16	56.35	-6.43	77.72	-14.66
3	HO ⁻ (H ₂ O) ₃ ···HCH ₂ CH ₂ ···Cl	15.19	23.30	33.11	6.36	38.49	8.11	56.41	-9.81	77.96	-18.64
4	HO ⁻ (H ₂ O) ₄ ···HCH ₂ CH ₂ ···Cl	16.49	23.65	32.90	6.19	40.14	7.16	56.55	-9.25	79.23	-19.55
0	HO ⁻ ···HCH ₂ CH ₂ ···Br	8.18	44.20	16.43	8.70	52.38	36.02	60.63	27.77	77.51	28.29
1	HO ⁻ (H ₂ O)···HCH ₂ CH ₂ ···Br	10.88	34.69	22.80	7.55	45.57	23.81	57.49	11.89	75.92	8.56
2	HO ⁻ (H ₂ O) ₂ ···HCH ₂ CH ₂ ···Br	13.63	28.96	27.24	6.61	42.59	15.33	56.20	1.72	76.44	-5.30
3	HO ⁻ (H ₂ O) ₃ ···HCH ₂ CH ₂ ···Br	14.08	27.21	28.76	6.38	41.29	13.13	55.97	-1.55	76.43	-9.25
4	HO ⁻ (H ₂ O) ₄ ···HCH ₂ CH ₂ ···Br	15.55	26.89	29.41	6.09	42.44	11.34	56.30	-2.52	77.94	-11.98
0	HO ⁻ ···HCH ₂ CH ₂ ···I	7.13	50.33	12.97	9.12	57.46	43.20	63.30	37.36	79.55	39.35
1	HO ⁻ (H ₂ O)···HCH ₂ CH ₂ ···I	9.94	39.40	19.30	7.83	49.34	29.46	58.70	20.10	76.47	17.99
2	HO ⁻ (H ₂ O) ₂ ···HCH ₂ CH ₂ ···I	12.47	32.79	23.75	6.85	45.26	20.32	56.54	9.04	75.86	3.42
3	HO ⁻ (H ₂ O) ₃ ···HCH ₂ CH ₂ ···I	12.96	30.70	25.36	6.62	43.66	17.74	56.06	5.34	75.64	-1.00
4	HO ⁻ (H ₂ O) ₄ ···HCH ₂ CH ₂ ···I	14.51	29.41	26.89	6.17	43.92	14.90	56.30	2.52	76.98	-18.16

Note: %^βC^βH[‡]_{E2}=100×($r^{\ddagger}_{\beta C-\beta H,E2} - r^{Reactant}_{\beta C-\beta H}$)/ $r^{Reactant}_{\beta C-\beta H}$. %CC[‡]_{E2}=100×($r^{\ddagger}_{C-C,E2} - r^{Product}_{C-C}$)/ $r^{Product}_{C-C}$. $r^{\ddagger}_{\beta C-\beta H,E2}$ and $r^{\ddagger}_{C-C,E2}$ are ^βC–^βH and C–C bond lengths in anti-E2 transition structure, and $r^{Product}_{C-C}$ is C–C bond length in product CH₂=CH₂.

$$\%L^{\ddagger}_{E2}(2) = \%^{\beta}HO^{\ddagger}_{E2} + \%^{\beta}C^{\beta}H^{\ddagger}_{E2}.$$

$$\%AS^{\ddagger}_{E2}(2) = \%^{\beta}HO^{\ddagger}_{E2} - \%^{\beta}C^{\beta}H^{\ddagger}_{E2}.$$

$$\%L^{\ddagger}_{E2}(3) = \%^aCX^{\ddagger}_{E2} + \%^{\beta}HO^{\ddagger}_{E2} + \%^{\beta}C^{\beta}H^{\ddagger}_{E2} + \%CC^{\ddagger}_{E2}.$$

$$\%AS^{\ddagger}_{E2}(3) = (\%^{\beta}HO^{\ddagger}_{E2} + \%CC^{\ddagger}_{E2}) - (\%^aCX^{\ddagger}_{E2} + \%^{\beta}C^{\beta}H^{\ddagger}_{E2}).$$

Table S15 NPA charge distributions for the inv-S_N2-TS. (X = Cl, Br, I)

n	Species	$q(\text{HO})$	$q(\text{O})$	$q(^{\text{a}}\text{C})$	$q(\text{X})$	$q(\text{CH}_2)$	$\Delta q(\text{X-O})$
0	$\text{HO}^- \cdots \text{CH}_3\text{CH}_2 \cdots \text{Cl}$	-0.862	-1.273	-0.061	-0.569	0.399	0.704
1	$\text{HO}^-(\text{H}_2\text{O}) \cdots \text{CH}_3\text{CH}_2 \cdots \text{Cl}$	-0.774	-1.205	-0.039	-0.611	0.420	0.594
2	$\text{HO}^-(\text{H}_2\text{O})_2 \cdots \text{CH}_3\text{CH}_2 \cdots \text{Cl}$	-0.738	-1.189	-0.010	-0.657	0.448	0.532
3	$\text{HO}^-(\text{H}_2\text{O})_3 \cdots \text{CH}_3\text{CH}_2 \cdots \text{Cl}$	-0.719	-1.174	-0.013	-0.658	0.446	0.516
4	$\text{HO}^-(\text{H}_2\text{O})_4 \cdots \text{CH}_3\text{CH}_2 \cdots \text{Cl}$	-0.706	-1.170	0.009	-0.699	0.468	0.471
0	$\text{HO}^- \cdots \text{CH}_3\text{CH}_2 \cdots \text{Br}$	-0.873	-1.284	-0.116	-0.516	0.356	0.768
1	$\text{HO}^-(\text{H}_2\text{O}) \cdots \text{CH}_3\text{CH}_2 \cdots \text{Br}$	-0.782	-1.214	-0.084	-0.567	0.384	0.646
2	$\text{HO}^-(\text{H}_2\text{O})_2 \cdots \text{CH}_3\text{CH}_2 \cdots \text{Br}$	-0.746	-1.197	-0.045	-0.622	0.420	0.575
3	$\text{HO}^-(\text{H}_2\text{O})_3 \cdots \text{CH}_3\text{CH}_2 \cdots \text{Br}$	-0.724	-1.179	-0.045	-0.628	0.421	0.551
4	$\text{HO}^-(\text{H}_2\text{O})_4 \cdots \text{CH}_3\text{CH}_2 \cdots \text{Br}$	-0.710	-1.175	-0.016	-0.675	0.447	0.499
0	$\text{HO}^- \cdots \text{CH}_3\text{CH}_2 \cdots \text{I}$	-0.885	-1.296	-0.202	-0.429	0.280	0.867
1	$\text{HO}^-(\text{H}_2\text{O}) \cdots \text{CH}_3\text{CH}_2 \cdots \text{I}$	-0.790	-1.221	-0.146	-0.502	0.327	0.720
2	$\text{HO}^-(\text{H}_2\text{O})_2 \cdots \text{CH}_3\text{CH}_2 \cdots \text{I}$	-0.751	-1.203	-0.093	-0.571	0.376	0.632
3	$\text{HO}^-(\text{H}_2\text{O})_3 \cdots \text{CH}_3\text{CH}_2 \cdots \text{I}$	-0.720	-1.184	-0.060	-0.627	0.409	0.557
4	$\text{HO}^-(\text{H}_2\text{O})_4 \cdots \text{CH}_3\text{CH}_2 \cdots \text{I}$	-0.712	-1.178	-0.046	-0.643	0.419	0.534

Table S16 NPA charge distributions for the anti-E2-TS. (X = Cl, Br, I)

n	Species	$q(\text{HO})$	$q(\text{O})$	$q(\beta\text{H})$	$q(\beta\text{C})$	$q(\text{CH}_2)$	$q(\text{X})$	$q(\text{CH}_2\text{CH}_2\text{X})$	$\Delta q(\text{X-O})$
0	$\text{HO}^- \cdots \text{CH}_3\text{CH}_2 \cdots \text{Cl}$	-0.812	-1.230	0.426	-0.772	0.202	-0.384	-0.614	0.845
1	$\text{HO}^-(\text{H}_2\text{O}) \cdots \text{CH}_3\text{CH}_2 \cdots \text{Cl}$	-0.733	-1.176	0.445	-0.799	0.211	-0.432	-0.665	0.743
2	$\text{HO}^-(\text{H}_2\text{O})_2 \cdots \text{CH}_3\text{CH}_2 \cdots \text{Cl}$	-0.709	-1.172	0.464	-0.808	0.233	-0.491	-0.699	0.681
3	$\text{HO}^-(\text{H}_2\text{O})_3 \cdots \text{CH}_3\text{CH}_2 \cdots \text{Cl}$	-0.701	-1.170	0.469	-0.809	0.224	-0.495	-0.711	0.675
4	$\text{HO}^-(\text{H}_2\text{O})_4 \cdots \text{CH}_3\text{CH}_2 \cdots \text{Cl}$	-0.715	-1.185	0.465	-0.824	0.254	-0.525	-0.709	0.660
0	$\text{HO}^- \cdots \text{CH}_3\text{CH}_2 \cdots \text{Br}$	-0.834	-1.249	0.416	-0.752	0.169	-0.347	-0.583	0.902
1	$\text{HO}^-(\text{H}_2\text{O}) \cdots \text{CH}_3\text{CH}_2 \cdots \text{Br}$	-0.748	-1.189	0.436	-0.780	0.183	-0.403	-0.637	0.785
2	$\text{HO}^-(\text{H}_2\text{O})_2 \cdots \text{CH}_3\text{CH}_2 \cdots \text{Br}$	-0.721	-1.183	0.455	-0.790	0.208	-0.465	-0.673	0.718
3	$\text{HO}^-(\text{H}_2\text{O})_3 \cdots \text{CH}_3\text{CH}_2 \cdots \text{Br}$	-0.714	-1.180	0.460	-0.791	0.202	-0.472	-0.685	0.709
4	$\text{HO}^-(\text{H}_2\text{O})_4 \cdots \text{CH}_3\text{CH}_2 \cdots \text{Br}$	-0.725	-1.195	0.458	-0.807	0.234	-0.511	-0.688	0.685
0	$\text{HO}^- \cdots \text{CH}_3\text{CH}_2 \cdots \text{I}$	-0.855	-1.267	0.413	-0.734	0.097	-0.263	-0.551	1.005
1	$\text{HO}^-(\text{H}_2\text{O}) \cdots \text{CH}_3\text{CH}_2 \cdots \text{I}$	-0.763	-1.201	0.426	-0.766	0.123	-0.335	-0.611	0.866
2	$\text{HO}^-(\text{H}_2\text{O})_2 \cdots \text{CH}_3\text{CH}_2 \cdots \text{I}$	-0.733	-1.193	0.446	-0.779	0.156	-0.406	-0.650	0.787
3	$\text{HO}^-(\text{H}_2\text{O})_3 \cdots \text{CH}_3\text{CH}_2 \cdots \text{I}$	-0.723	-1.188	0.452	-0.782	0.150	-0.413	-0.664	0.774
4	$\text{HO}^-(\text{H}_2\text{O})_4 \cdots \text{CH}_3\text{CH}_2 \cdots \text{I}$	-0.730	-1.201	0.452	-0.794	0.188	-0.470	-0.676	0.731

Table S17 Energy decomposition analysis of inv-S_N2 and anti-E2 transition structure at MP2/ECP/d level.

kcal/mol	ΔE^\ddagger	ΔE_{int}	ΔE_{prep}			ΔE^\ddagger	ΔE_{int}	ΔE_{prep}		
			overall	$\text{HO}^-(\text{H}_2\text{O})_n$	$\text{CH}_3\text{CH}_2\text{X}$			overall	$\text{HO}^-(\text{H}_2\text{O})_n$	$\text{CH}_3\text{CH}_2\text{X}$
inv-S_N2, X = Cl										
0	-13.1	-28.6	15.5	0.0	15.5	-13.2	-31.8	18.6	0.0	18.6
1	-6.2	-27.3	21.1	0.8	20.3	-4.2	-34.2	30.0	1.6	28.4
2	-1.0	-27.4	26.4	1.1	25.3	3.2	-36.6	39.8	2.7	37.1
3	4.7	-28.9	33.6	7.2	26.4	10.4	-37.3	47.7	8.1	39.6
4	9.9	-30.4	40.3	8.9	31.5	14.0	-39.6	53.6	10.9	42.7
anti-E2, X = Cl										
inv-S_N2, X = Br										
0	-15.8	-27.5	11.7	0.0	11.7	-15.2	-29.5	14.3	0.0	14.3
1	-9.0	-26.1	17.1	0.8	16.3	-6.7	-31.3	24.7	1.4	23.3
2	-3.9	-26.2	22.3	1.1	21.2	0.4	-33.2	33.6	2.4	31.2
3	1.7	-27.8	29.6	6.9	22.6	7.4	-34.0	41.4	7.9	33.5
4	6.9	-26.1	33.0	9.5	23.5	10.8	-36.6	47.4	10.0	37.4
anti-E2, X = Br										
inv-S_N2, X = I										
0	-17.8	-26.1	8.3	0.0	8.3	-16.7	-27.1	10.4	0.0	10.3
1	-10.8	-24.6	13.8	0.9	12.9	-8.6	-28.5	19.9	1.4	18.5
2	-5.7	-24.7	19.0	1.2	17.8	-1.8	-30.1	28.2	2.3	25.9
3	-0.1	-25.2	25.1	2.4	22.7	5.2	-30.4	35.5	7.4	28.1
4	5.5	-27.4	32.9	8.5	24.4	8.7	-33.3	42.0	9.4	32.6
anti-E2, X = I										

Table S18 Selected bond distances (\AA) of inv-S_N2-TS and anti-E2-TS structures for $\text{HO}^-(\text{H}_2\text{O})_{n=0-4} + \text{CH}_3\text{CH}_2\text{X}$ ($\text{X} = \text{Cl}, \text{Br}, \text{I}$) reactions as optimized by PCM(water)-MP2/ECP/d method.

inv-S _N 2-TS					anti-E2-TS				
X	n	$r(\text{O}-{}^a\text{C})$	$r({}^a\text{C}-\text{X})$	$r(\text{O}-\text{X})$	$r({}^a\text{C}-{}^{\beta}\text{C})$	$r(\text{O}-{}^{\beta}\text{H})$	$r({}^a\text{C}-\text{X})$	$r({}^{\beta}\text{H}-{}^{\beta}\text{C})$	$r({}^a\text{C}-{}^{\beta}\text{C})$
Cl	0	2.190	2.168	4.335	1.509	1.272	2.035	1.378	1.450
	1	2.152	2.197	4.325	1.509	1.264	2.085	1.385	1.439
	2	2.122	2.225	4.323	1.509	1.269	2.145	1.381	1.428
	3	2.117	2.230	4.323	1.509	1.268	2.147	1.381	1.427
	4	2.095	2.253	4.324	1.510	1.211	2.075	1.446	1.441
Br	0	2.210	2.295	4.479	1.509	1.302	2.189	1.350	1.448
	1	2.169	2.325	4.467	1.510	1.288	2.233	1.363	1.439
	2	2.137	2.355	4.463	1.510	1.285	2.284	1.364	1.429
	3	2.138	2.353	4.464	1.510	1.286	2.288	1.365	1.428
	4	2.105	2.383	4.462	1.510	1.295	2.282	1.356	1.430
I	0	2.221	2.486	4.676	1.511	1.321	2.392	1.333	1.451
	1	2.177	2.517	4.663	1.512	1.441	2.431	1.350	1.441
	2	2.144	2.548	4.659	1.511	1.295	2.478	1.355	1.432
	3	2.143	2.548	4.659	1.512	1.295	2.481	1.356	1.432
	4	2.110	2.581	4.660	1.511	1.304	2.475	1.349	1.432

Table 19 Calculated overall barrier of inv-S_N2 and anti-E2 transition states using different models. MP2/ECP/d method was used.

	kcal/m ol	inv-S _N 2			anti-E2			^d ΔΔE [‡] (antiE2-invS _N 2)		
		X	Cl ΔE^{\ddagger}	Br ΔE^{\ddagger}	I ΔE^{\ddagger}	Cl ΔE^{\ddagger}	Br ΔE^{\ddagger}	I ΔE^{\ddagger}	Cl	Br
^a PCM/OPT	n = 0	11.5	10.1	9.8	13.4	12.1	11.5	1.9	2.0	1.6
	n = 1	11.8	10.4	10.1	16.3	14.7	13.9	4.5	4.3	3.8
	n = 2	12.4	10.9	10.6	19.1	17.2	16.3	6.7	6.4	5.7
	n = 3	13.8	12.0	12.1	20.1	18.1	17.1	6.2	6.0	5.0
	n = 4	14.2	12.3	12.4	22.0	18.5	17.6	7.8	6.1	5.3
^b PCM/SP	n = 0	11.4	9.8	9.1	12.5	10.7	9.2	1.1	0.8	0.1
	n = 1	11.6	10.1	9.7	16.1	14.3	13.1	4.5	4.2	3.3
	n = 2	13.0	11.6	11.5	19.5	17.7	16.8	6.5	6.1	5.3
	n = 3	13.0	11.4	11.8	22.4	20.3	19.5	9.4	8.9	7.7
	n = 4	13.1	11.4	11.6	22.4	20.1	19.1	9.3	8.7	7.5
^c ΔE [‡] (PCM/OPT) -ΔE [‡] (PCM/SP)	n = 0	0.1	0.3	0.7	0.9	1.4	2.3	0.8	1.2	1.5
	n = 1	0.2	0.3	0.4	0.2	0.4	0.8	0	0.1	0.5
	n = 2	-0.6	-0.7	-0.9	-0.4	-0.5	-0.5	0.2	0.3	0.4
	n = 3	0.8	0.6	0.3	-2.3	-2.2	-2.4	-3.2	-2.9	-2.7
	n = 4	1.1	0.9	0.8	-0.4	-1.6	-1.5	-1.5	-2.6	-2.2

^aPCM/OPT refers to structures were optimized in PCM solvent model with water as solvent.

^bPCM/SP refers to single point energies using PCM solvent model computed on top of gas-phase optimized structures.

^cΔE[‡](PCM/OPT) -ΔE[‡](PCM/SP) refers to barrier difference between PCM-OPT and PCM-SP models. Values that are greater than 1 kcal/mol are in bold.

^dΔΔE[‡](antiE2-invS_N2) refers to the barrier difference between anti-E2 TS and inv-S_N2 TS.

Effect of PCM solvent model

To evaluate the contribution of ΔE_{ee} and ΔE_{geo} , we computed single point energy using PCM implicit solvent model on top of the gas-phase optimized structure. This energy is denoted as $E_{PCM/SP}$, to distinguish it from the energies of structures optimized in PCM ($E_{PCM/OPT}$) and optimized in gas-phase (E_{GAS}). And the respective energies can be calculated as following.

$$\Delta E_{PCM-GAS} = E_{PCM/OPT} - E_{GAS}$$

$$\Delta E_{ee} = E_{PCM/SP} - E_{GAS}$$

$$\Delta E_{geo} = \Delta E_{PCM-GAS} - \Delta E_{ee} = \Delta E_{PCM-GAS} - E_{PCM/SP}$$

Above energetic terms were computed for reactants and transition states (Table S20) and their differences were calculated to evaluate the contribution from ΔE_{ee} and ΔE_{geo} to barrier heights (Table S21).

$$\Delta\Delta E^\ddagger_{PCM-GAS} = \Delta E_{PCM-GAS}(\text{transition state}) - \Delta E_{PCM-GAS}(\text{reactants})$$

$$\Delta\Delta E^\ddagger_{ee} = \Delta E_{ee}(\text{transition state}) - \Delta E_{ee}(\text{reactants})$$

$$\Delta\Delta E^\ddagger_{geo} = \Delta E_{geo}(\text{transition state}) - \Delta E_{geo}(\text{reactants})$$

Table 20 Energy differences between gas-phase and PCM calculations and the compositions.

kcal/mol	species	^a $\Delta E_{\text{PCM-GAS}}$	^b ΔE_{ee}	^c ΔE_{geo}
Reactant	HO^-	-79.965	-79.961	-0.003
	$\text{HO}^-(\text{H}_2\text{O})$	-69.627	-69.204	-0.422
	$\text{HO}^-(\text{H}_2\text{O})_2$	-62.798	-62.265	-0.533
	$\text{HO}^-(\text{H}_2\text{O})_3$	-57.695	-56.622	-1.073
	$\text{HO}^-(\text{H}_2\text{O})_4$	-52.650	-51.614	-1.036
	$\text{CH}_3\text{CH}_2\text{Cl}$	-2.069	-2.032	-0.037
	$\text{CH}_3\text{CH}_2\text{Br}$	-1.949	-1.925	-0.024
	$\text{CH}_3\text{CH}_2\text{I}$	-1.698	-1.684	-0.014
X n				
inv-S_N2 TS	Cl 0	-57.427	-57.431	0.004
	1	-53.704	-53.423	-0.280
	2	-51.448	-50.324	-1.124
	3	-50.604	-50.284	-0.320
	4	-50.487	-50.479	-0.008
	Br 0	-55.982	-56.201	0.219
	1	-52.253	-52.035	-0.218
	2	-49.977	-48.707	-1.270
	3	-49.348	-48.914	-0.433
	4	-49.134	-48.988	-0.146
	I 0	-53.992	-54.745	0.753
	1	-50.279	-50.225	-0.054
	2	-48.029	-46.627	-1.401
	3	-47.070	-46.262	-0.808
	4	-47.305	-46.987	-0.319
anti-E2 TS	Cl 0	-55.408	-56.265	0.857
	1	-51.211	-50.922	-0.288
	2	-48.969	-48.006	-0.963
	3	-50.065	-46.613	-3.452
	4	-46.683	-45.216	-1.467
	Br 0	-54.617	-55.997	1.380
	1	-50.232	-50.163	-0.069
	2	-47.891	-46.864	-1.027
	3	-48.982	-45.663	-3.320
	4	-46.926	-44.249	-2.677
	I 0	-53.438	-55.741	2.302
	1	-48.728	-49.114	0.386
	2	-46.197	-45.234	-0.962
	3	-47.311	-43.829	-3.482
	4	-45.229	-42.649	-2.580

^a $\Delta E_{\text{PCM-GAS}} = E_{\text{PCM-OPT}} - E_{\text{GAS}}$

^b $\Delta E_{\text{ee}} = E_{\text{PCM-SP}} - E_{\text{GAS}}$

^c $\Delta E_{\text{geo}} = \Delta E_{\text{PCM-GAS}} - \Delta E_{\text{ee}}$

Table 21 Barrier differences between gas-phase and PCM calculations and the compositions.

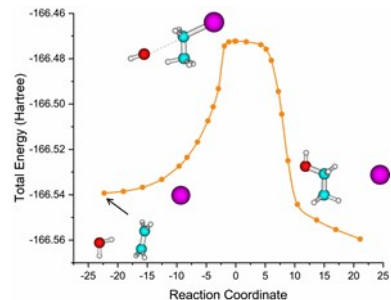
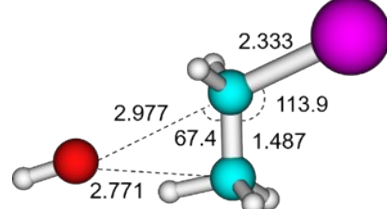
kcal/mol	species		^a $\Delta\Delta E^\ddagger_{\text{PCM-GAS}}$	^b $\Delta\Delta E^\ddagger_{\text{ee}}$	^c $\Delta\Delta E^\ddagger_{\text{geo}}$
	X	n			
inv-S_N2 TS	Cl	0	24.607	24.562	0.044
		1	17.992	17.813	0.179
		2	13.419	13.973	-0.554
		3	9.160	8.370	0.790
		4	4.232	3.167	1.065
	Br	0	25.932	25.685	0.246
		1	19.323	19.094	0.228
		2	14.770	15.483	-0.713
		3	10.296	9.633	0.664
		4	5.465	4.551	0.914
	I	0	27.671	26.900	0.770
		1	21.046	20.663	0.382
		2	16.467	17.322	-0.854
		3	12.323	12.044	0.279
		4	7.043	6.311	0.731
anti-E2 TS	Cl	0	26.626	25.728	0.897
		1	20.485	20.314	0.171
		2	15.898	16.291	-0.393
		3	9.699	12.041	-2.342
		4	8.036	8.430	-0.394
	Br	0	27.297	25.889	1.407
		1	21.344	20.966	0.377
		2	16.856	17.326	-0.470
		3	10.662	12.884	-2.223
		4	7.673	9.290	-1.617
	I	0	28.225	25.904	2.319
		1	22.597	21.774	0.822
		2	18.299	18.715	-0.415
		3	12.082	14.477	-2.395
		4	9.119	10.649	-1.530

^a $\Delta\Delta E^\ddagger_{\text{PCM-GAS}} = \Delta E_{\text{PCM-GAS}}(\text{transition state}) - \Delta E_{\text{PCM-GAS}}(\text{reactants})$

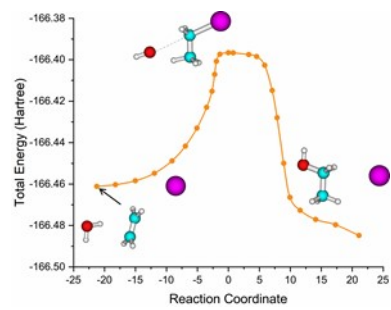
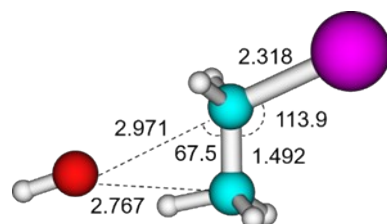
^b $\Delta\Delta E^\ddagger_{\text{ee}} = \Delta E_{\text{ee}}(\text{transition state}) - \Delta E_{\text{PCM/GAS}}(\text{reactants})$

^c $\Delta\Delta E^\ddagger_{\text{geo}} = \Delta E_{\text{geo}}(\text{transition state}) - \Delta E_{\text{geo}}(\text{reactants})$

a. B3LYP



b. B97-1



c. OLYP

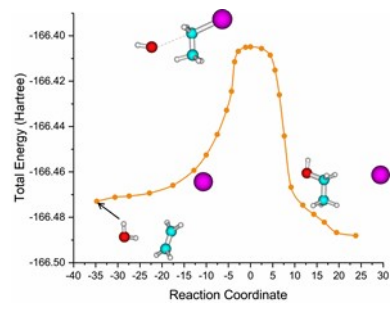
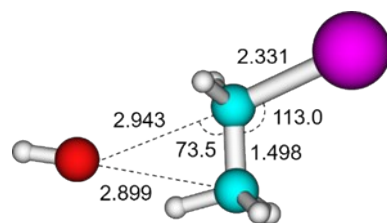


Figure S1. Intrinsic reaction coordinates (IRC) calculation of the anti-E2-TS/inv-S_N2-TS of HO⁻ + CH₃CH₂I S_N2 reaction using **a)** B3LYP, **b)** B97-1, and **c)** OLYP functional with ECP/d basis set.

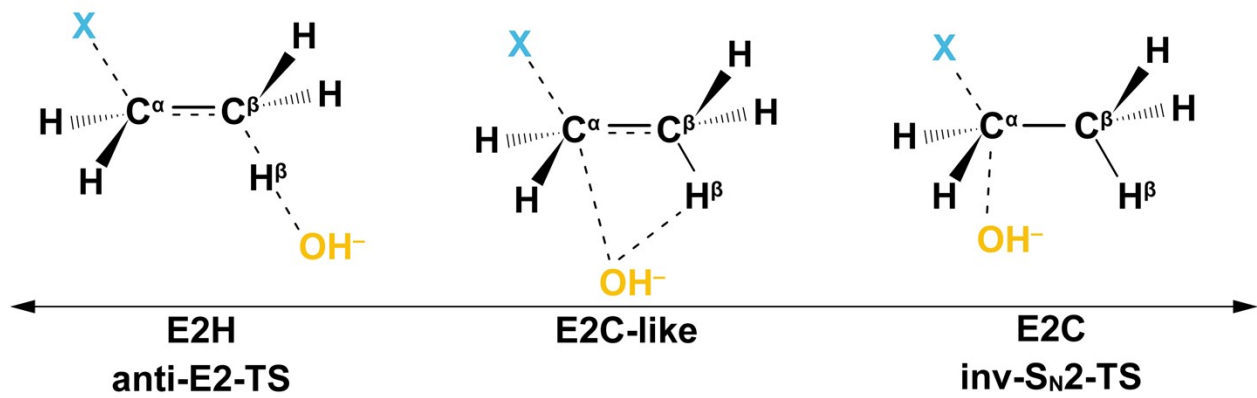


Figure S2. Mechanic spectra of the competing bimolecular nucleophilic substitution ($\text{S}_{\text{N}}2$) reaction vs. bimolecular elimination (E2) reaction.

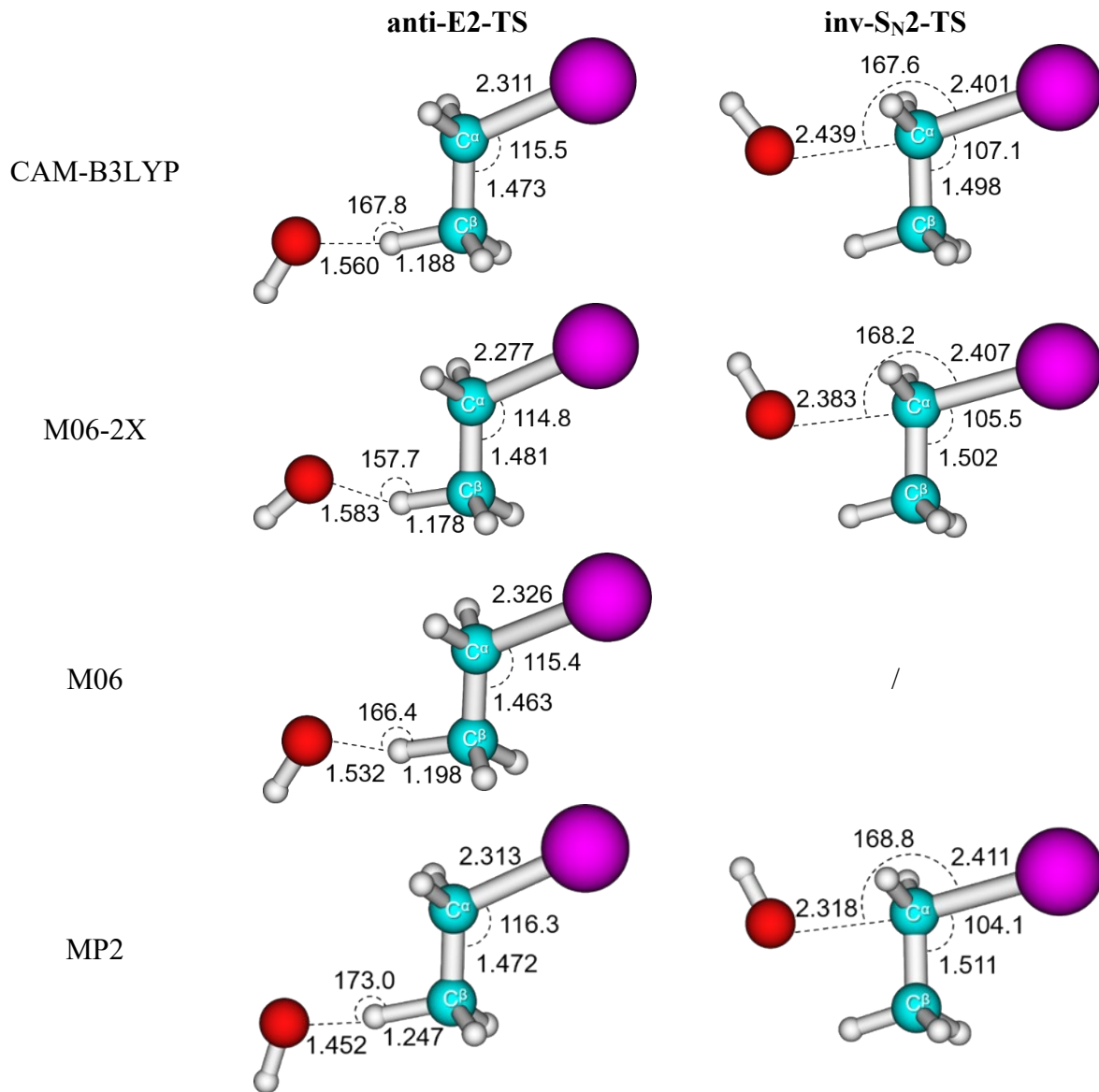
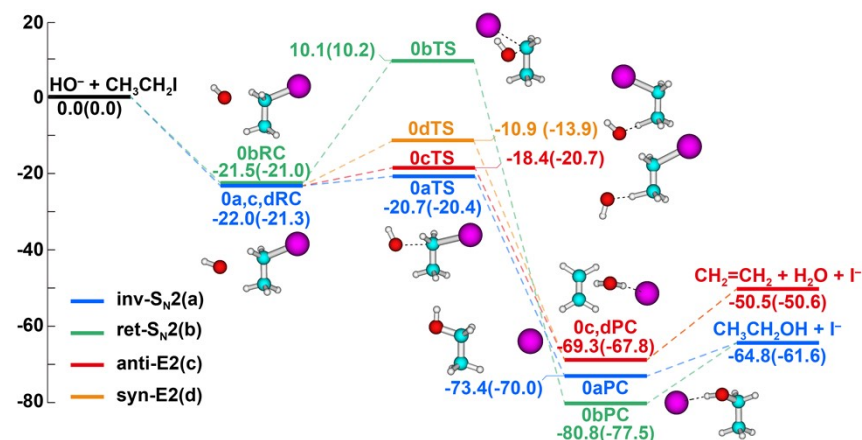


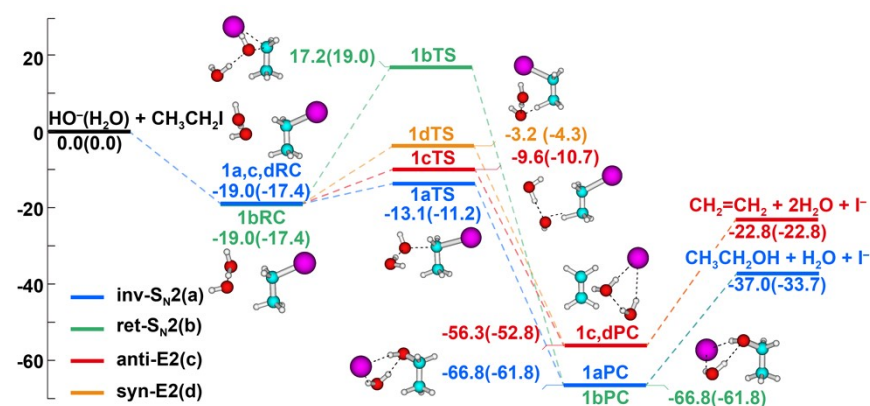
Figure S3. Structure comparison of anti-E2-TS and inv-S_N2-TS optimized by CAM-B3LYP, M06-2X, M06, and MP2 method with ECP/d basis set. Bond distances are in Å and bond angles are in degree. Color code: H, white; C, blue; O, red; I, purple.

Note: As shown in Figure S3, for inv-S_N2-TS, the O—C^α—I is close to linear (167.6°, CAM-B3LYP; 168.2°, M06-2X; 168.8°, MP2), signifying the nucleophilic attack on the C^α atom, and the respective imaginary frequencies are -265.1, -295.7, and -380.2 cm⁻¹. Whereas for anti-E2-TS structure, the O—H—C^β is close to linear (167.8°, CAM-B3LYP; 157.7°, M06-2X; 173.0°, MP2), signifying the nucleophilic attack on H atom, and the respective imaginary frequencies are -185.2, -202.0, and -570.7 cm⁻¹.

a. $n = 0$



b. $n = 1$



c. $n = 2$

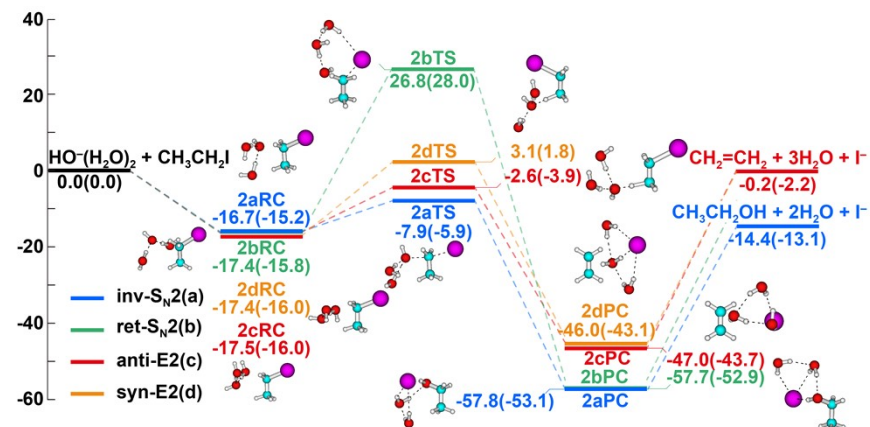
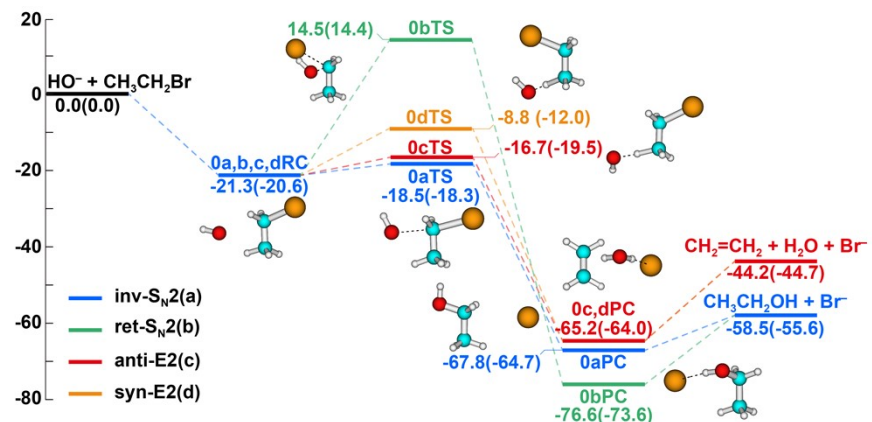
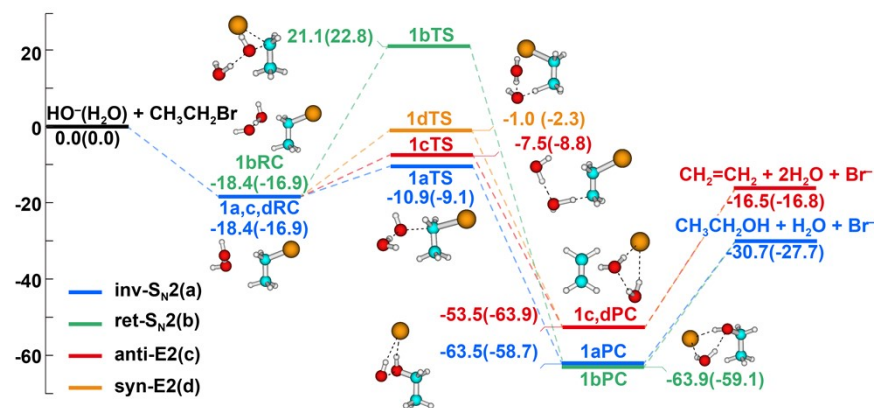


Figure S4 The potential energy profiles of $\text{S}_{\text{N}}2$ and E2 channels of $\text{HO}^-(\text{H}_2\text{O})_{n=0,1,2} + \text{CH}_3\text{CH}_2\text{I}$ reactions. The energies (in kcal/mol) in normal text are obtained at the CCSD(T)/PP/t level of theory, and enthalpy values at 298.15 K are in parentheses. Color code: H, white; C, blue; O, red; I, purple.

a. $n = 0$



b. $n = 1$



c. $n = 2$

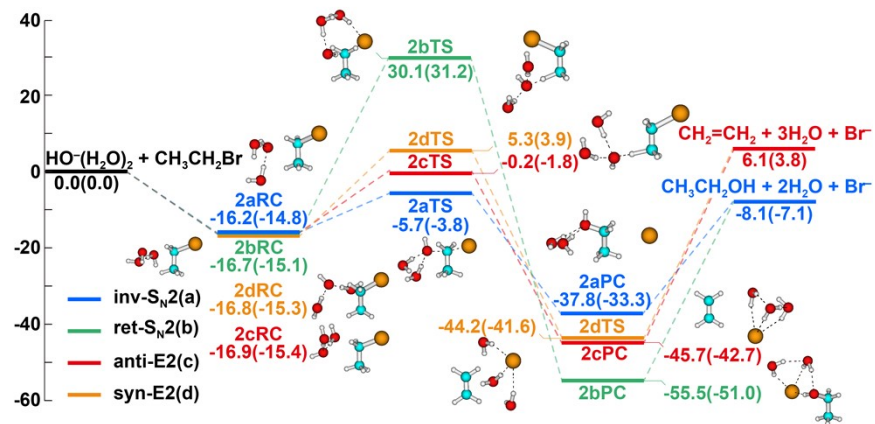
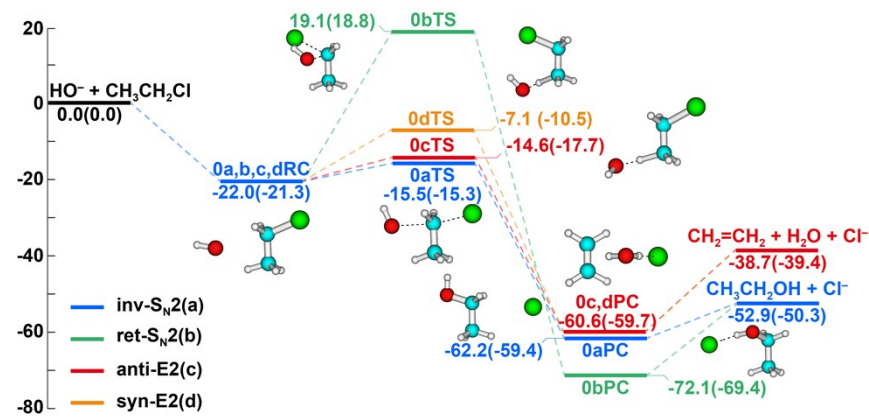
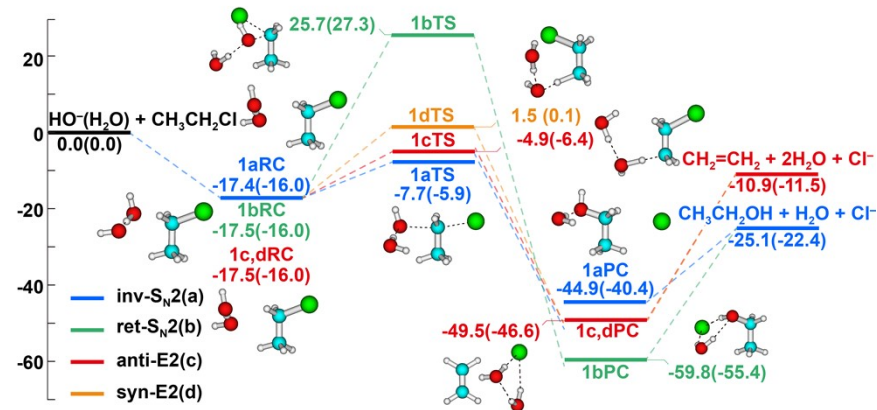


Figure S5 The potential energy profiles of S_N2 and E2 channels of $\text{HO}^-(\text{H}_2\text{O})_{n=0,1,2} + \text{CH}_3\text{CH}_2\text{Br}$ reactions. The energies (in kcal/mol) in normal text are obtained at the CCSD(T)/PP/t level of theory, and enthalpy values at 298.15 K are in parentheses. Color code: H, white; C, blue; O, red; Br, orange.

a. $n = 0$



b. $n = 1$



c. $n = 2$

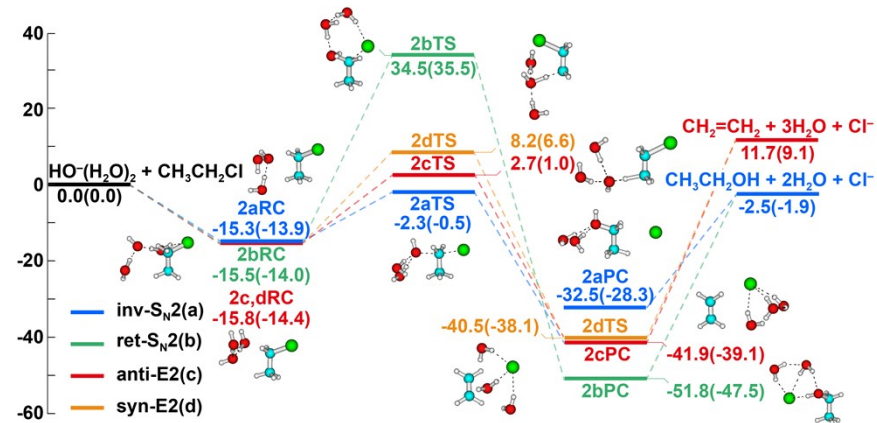
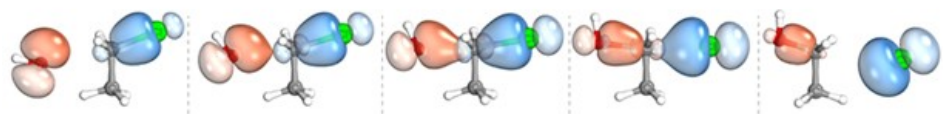
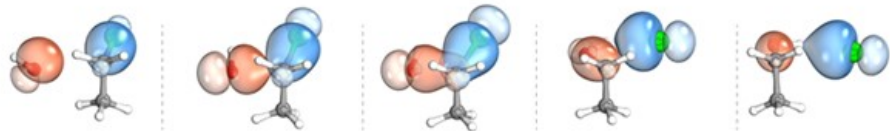


Figure S6 The potential energy profiles of $\text{S}_{\text{N}}2$ and E2 channels of $\text{HO}^-(\text{H}_2\text{O})_{n=0,1,2} + \text{CH}_3\text{CH}_2\text{Cl}$ reactions. The energies (in kcal/mol) in normal text are obtained at the CCSD(T)/PP/t level of theory, and enthalpy values at 298.15 K are in parentheses. Color code: H, white; C, blue; O, red; Cl, green.

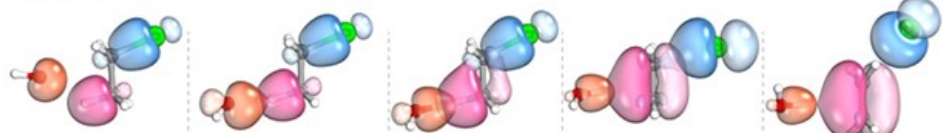
a. inv-S_N2



b. ret-S_N2



c. anti-E2



d. syn-E2

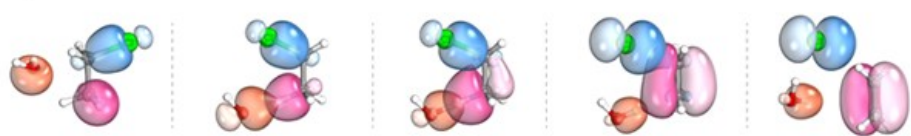
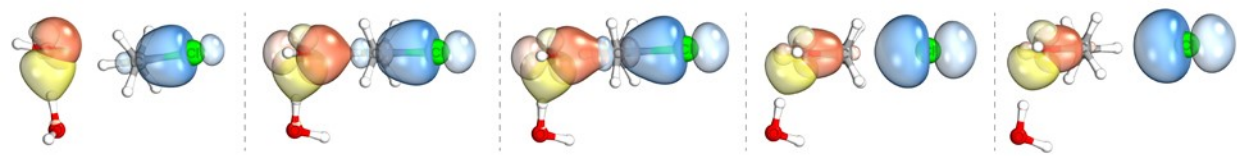
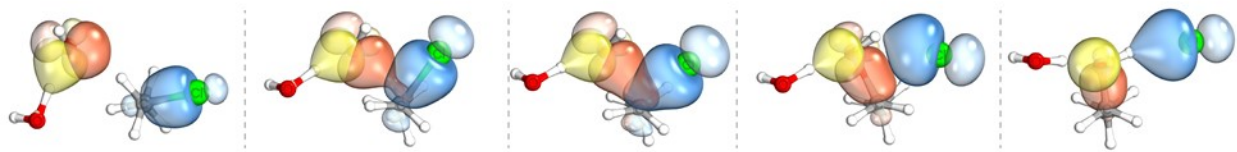


Figure S7 The intrinsic bond orbitals (IBOs)^{24, 25} of reactive orbitals of the (a) inv-S_N2, (b)ret-S_N2, (c) anti-E2-TS, (d) syn-E2-TS pathways of HO⁻ + CH₃CH₂Cl reaction. Element color code: H, white; C, grey; O, red; Cl, green.

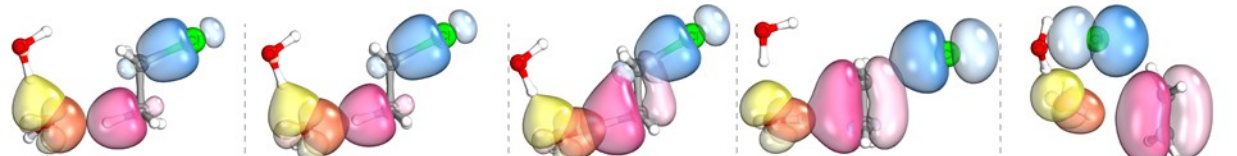
a. inv-S_N2



b. ret-S_N2



c. anti-E2



d. syn-E2

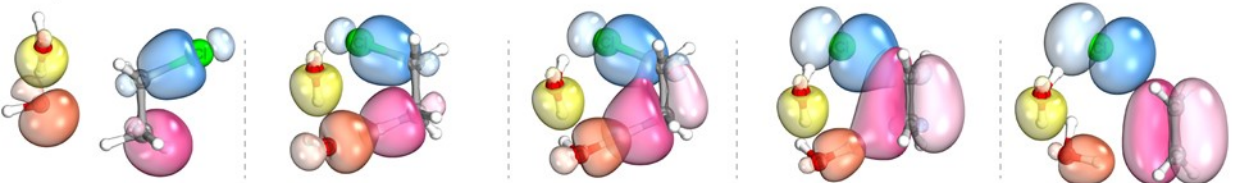
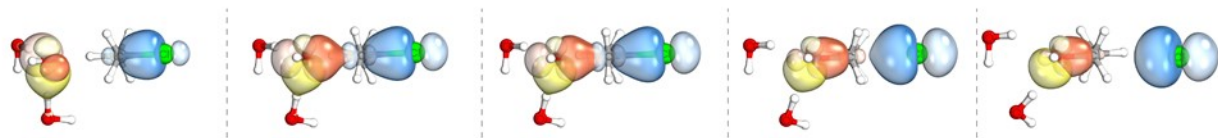
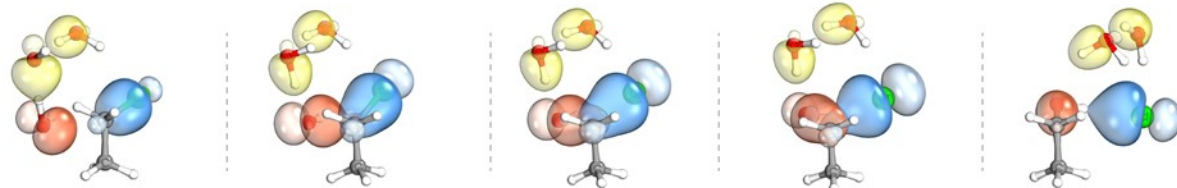


Figure S8 The IBOs²⁵ of reactive orbitals of the HO⁻(H₂O) + CH₃CH₂Cl reactions.

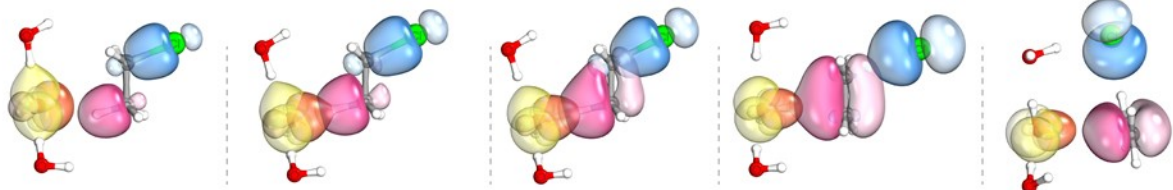
a. inv- S_N2



b. ret- S_N2



c. anti-E2



d. syn-E2

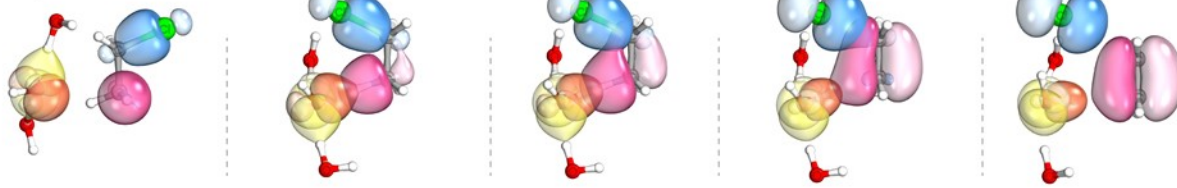


Figure S9 The IBOs²⁵ of reactive orbitals of the $\text{HO}^-(\text{H}_2\text{O})_2 + \text{CH}_3\text{CH}_2\text{Cl}$ reactions.

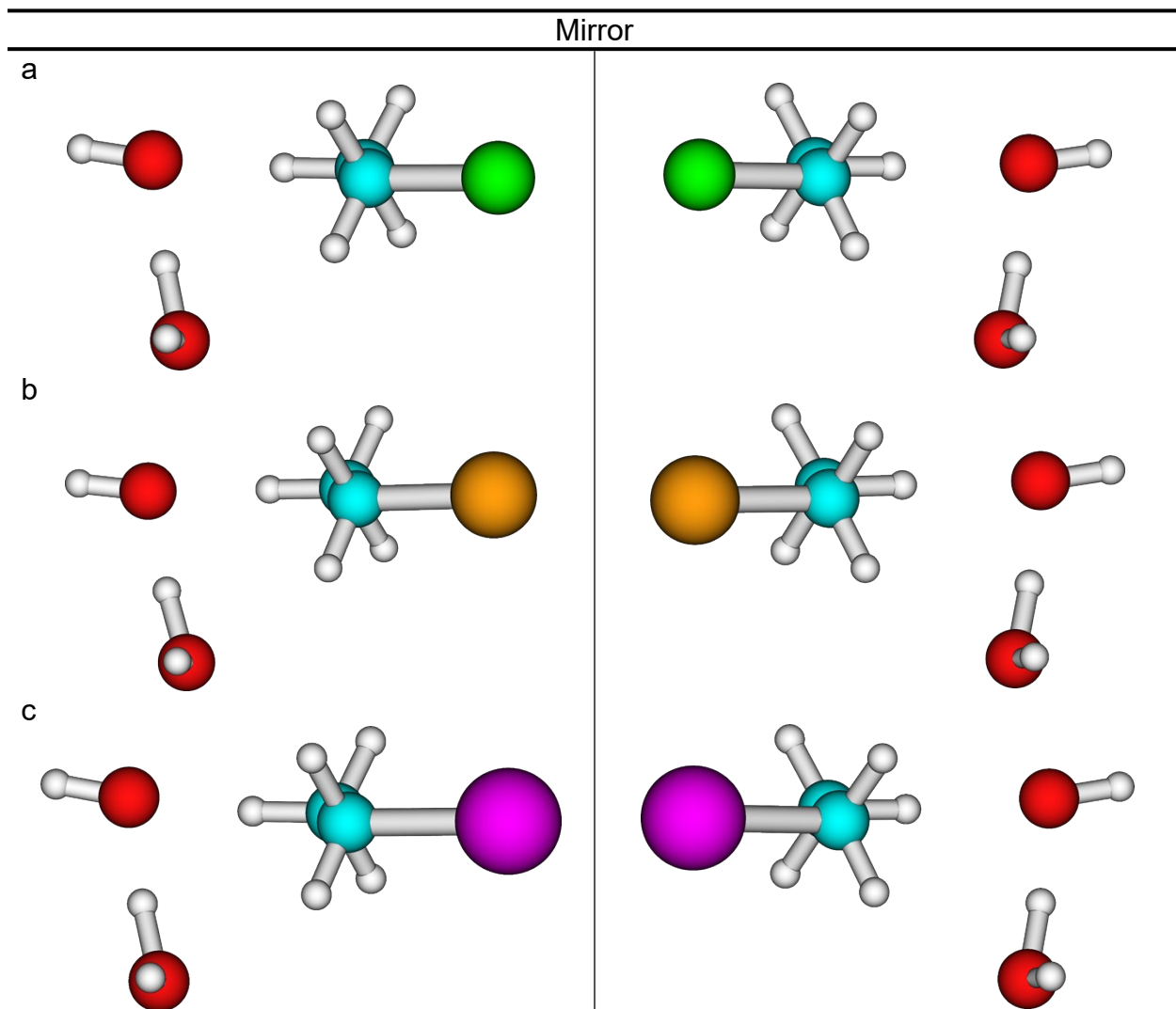


Figure S10 Mirror images of the pre-reaction complexes of $\text{HO}^-(\text{H}_2\text{O}) + \text{CH}_2\text{CH}_3\text{X}$ reactions.
Color code: H, white; C, blue; O, red; Cl, green; Br, orange; I, purple.

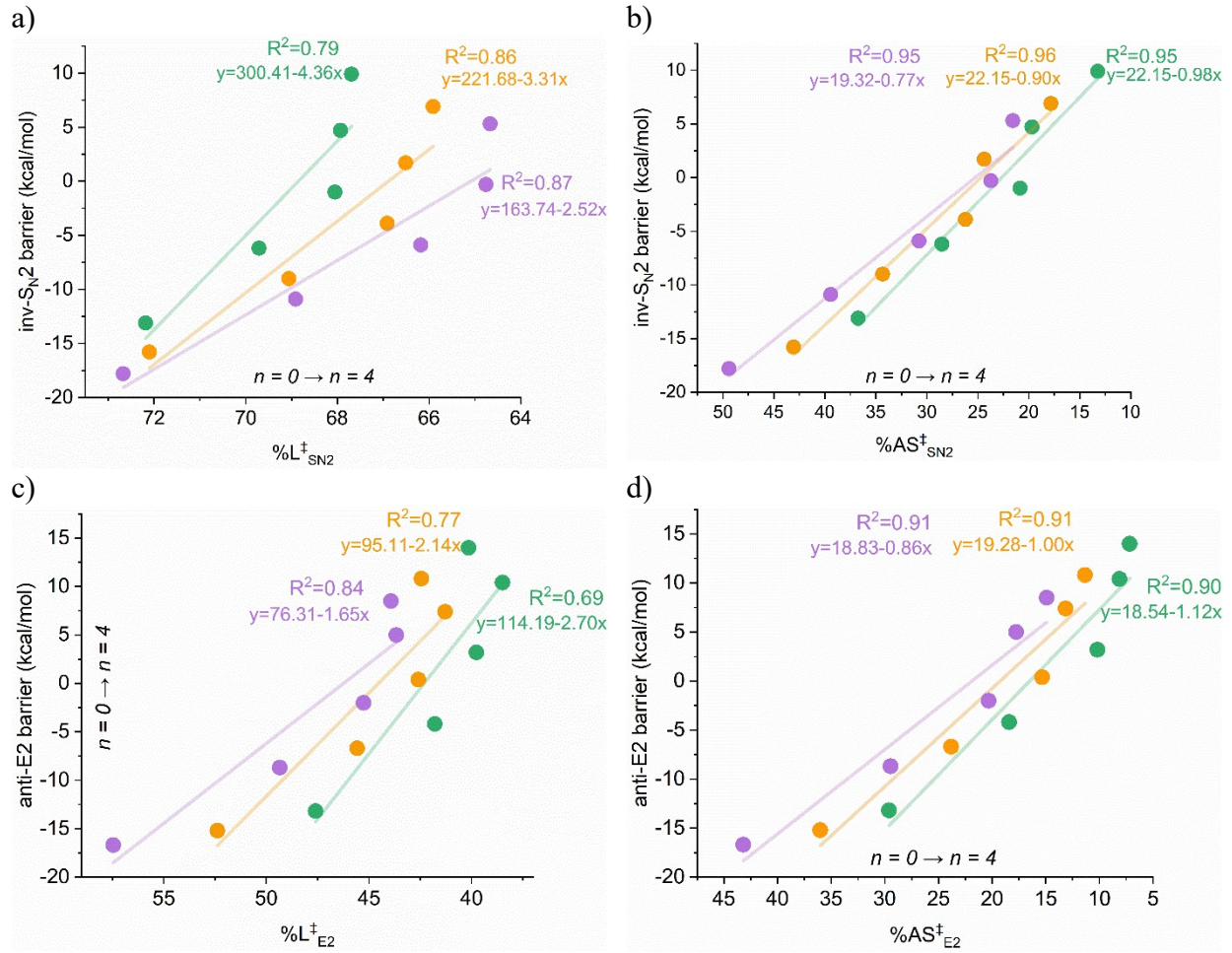


Figure S11. Plots of inv-S_N2 barrier heights vs a) %L[‡]_{SN2} and b) %AS[‡]_{SN2}, and anti-E2 barrier heights vs c) %L[‡]_{E2} and d) %AS[‡]_{E2}. (color code: green, CH₃CH₂Cl, orange, CH₃CH₂Br, purple, CH₃CH₂I)

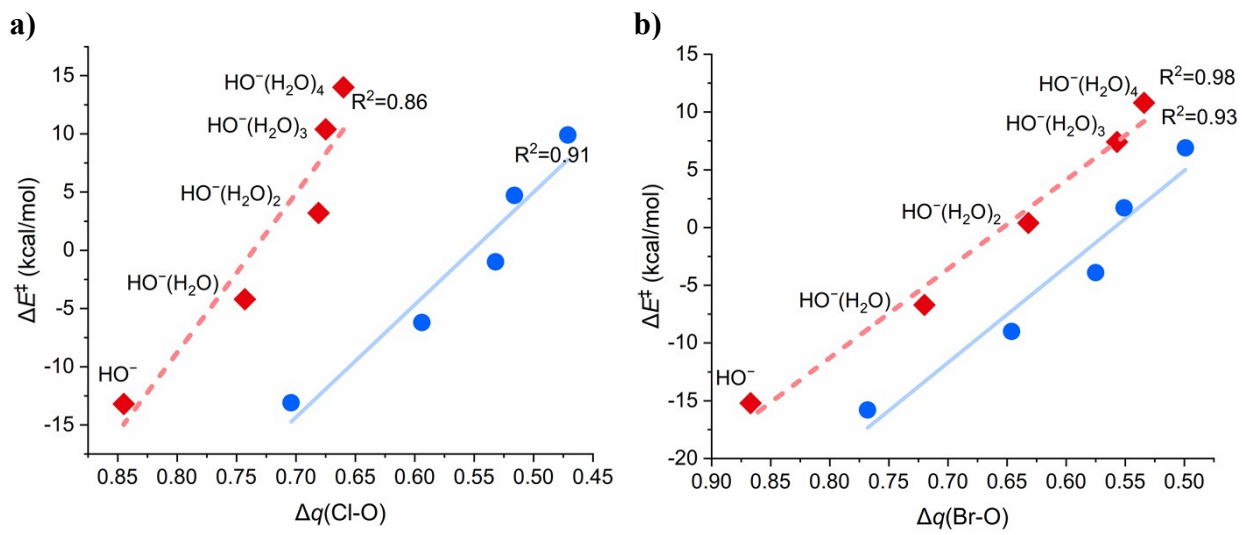


Figure S12. Plots of inv- $\text{S}_{\text{N}}2$ and anti- $\text{S}_{\text{N}}2$ barrier heights vs asymmetry of charge distribution $\Delta q(\text{X}-\text{O})$ for a) $\text{X} = \text{Cl}$ and b) $\text{X} = \text{Br}$. (color code: green, $\text{CH}_3\text{CH}_2\text{Cl}$, orange, $\text{CH}_3\text{CH}_2\text{Br}$, purple, $\text{CH}_3\text{CH}_2\text{I}$)

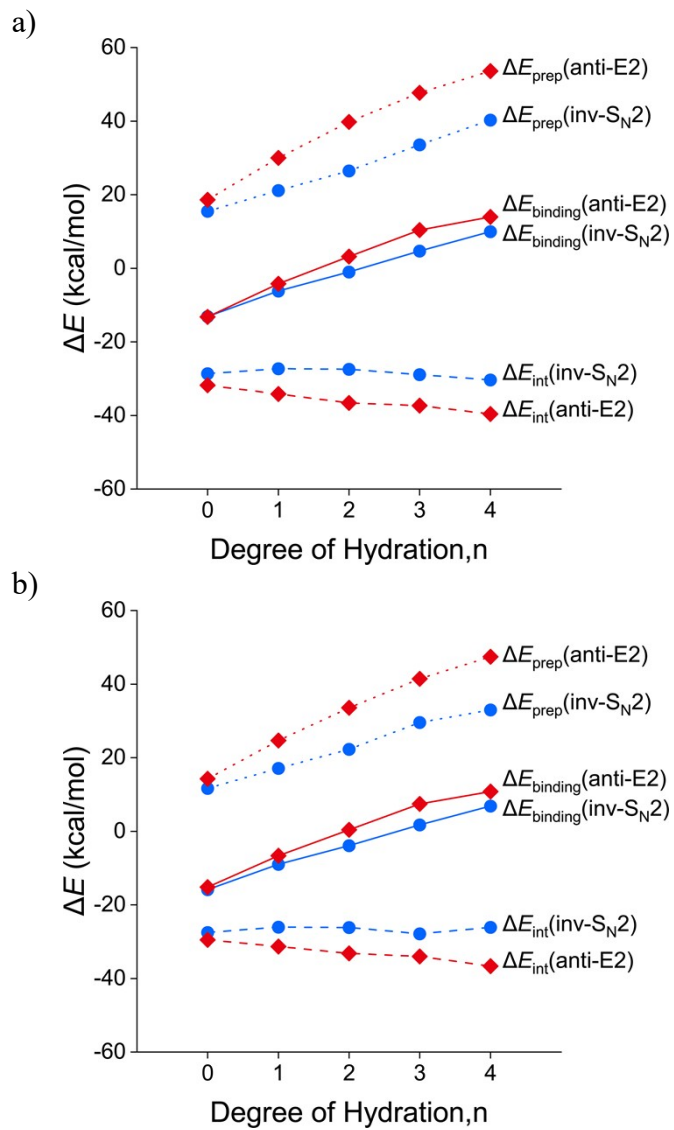
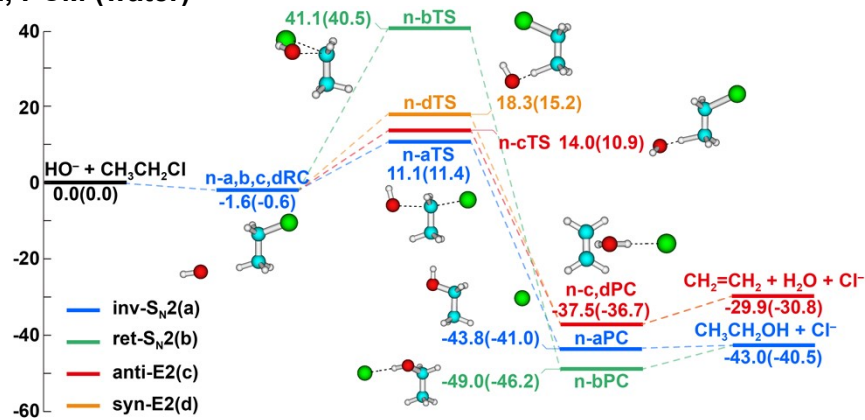
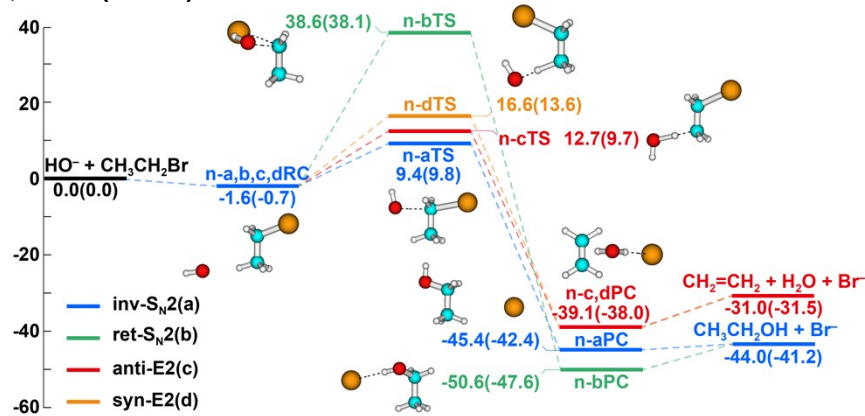


Figure S13. Energy decomposition analysis of inv-S_N2 and anti-E2 transition structure between HO⁻(H₂O)_n and a) CH₃CH₂Cl and b) CH₃CH₂Br.

a. X = Cl, PCM (water)



b. X = Br, PCM (water)



c. X = I, PCM (water)

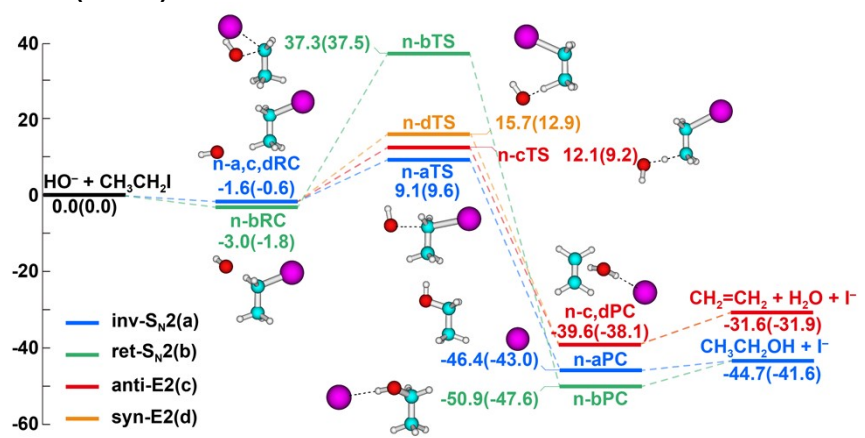


Figure S14 The potential energy profiles of $\text{S}_{\text{N}}2$ and E2 reactions of $\text{HO}^- + \text{CH}_3\text{CH}_2\text{X}$ ($\text{X} = \text{Cl}, \text{Br}, \text{I}$) as calculated using implicit PCM solvent model with water as the solvent. The energies (in kcal/mol) in normal text are obtained at the CCSD(T)/PP/t level of theory, and enthalpy values at 298.15 K are in parentheses. Color code: H, white; C, blue; O, red; Cl, green; Br, orange; I, purple.

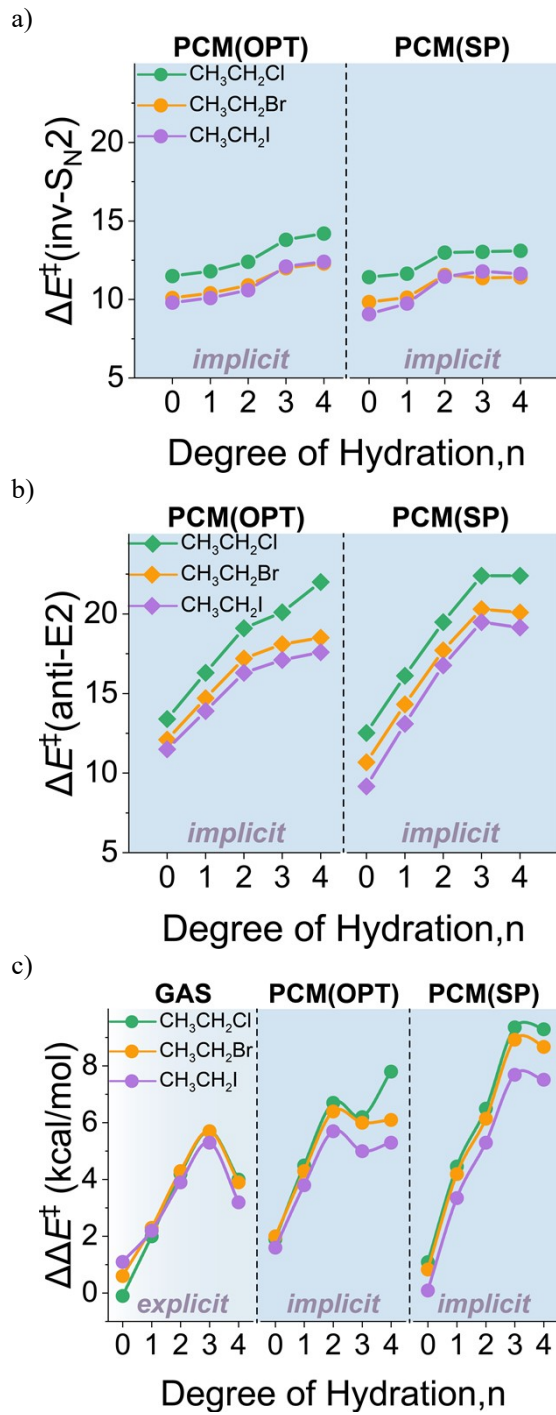


Figure S15 Comparison of barrier heights of a) inv- S_N2 and b) anti-E2 transition states and c) barrier difference $\Delta\Delta E^\ddagger$ between gas-phase, PCM, and PCM-SP methods.

Reference

1. T. Minato and S. Yamabe, *Journal of the American Chemical Society*, 1988, **110**, 4586-4593.
2. S. Gronert, *Journal of the American Chemical Society*, 1991, **113**, 6041-6048.
3. F. M. Bickelhaupt, E. J. Baerends, N. M. M. Nibbering and T. Ziegler, *Journal of the American Chemical Society*, 1993, **115**, 9160-9173.
4. G. N. Merrill, S. Gronert and S. R. Kass, *The Journal of Physical Chemistry A*, 1997, **101**, 208-218.
5. M. Mugnai, G. Cardini and V. Schettino, *The Journal of Physical Chemistry A*, 2003, **107**, 2540-2547.
6. A. P. Bento, M. Solà and F. M. Bickelhaupt, *Journal of Chemical Theory and Computation*, 2008, **4**, 929-940.
7. Y. Zhao and D. G. Truhlar, *Journal of Chemical Theory and Computation*, 2010, **6**, 1104-1108.
8. M. Swart, M. Solà and F. M. Bickelhaupt, *Journal of Chemical Theory and Computation*, 2010, **6**, 3145-3152.
9. L. Yang, J. Zhang, J. Xie, X. Ma, L. Zhang, C. Zhao and W. L. Hase, *The Journal of Physical Chemistry A*, 2017, **121**, 1078-1085.
10. V. Tajti and G. Czakó, *The Journal of Physical Chemistry A*, 2017, **121**, 2847-2854.
11. E. Carrascosa, J. Meyer, J. Zhang, M. Stei, T. Michaelsen, W. L. Hase, L. Yang and R. Wester, *Nature Communications*, 2017, **8**, 25.
12. L. Satpathy, P. K. Sahu, P. K. Behera and B. K. Mishra, *The Journal of Physical Chemistry A*, 2018, **122**, 5861-5869.
13. Y. Zhao and D. G. Truhlar, *Accounts of Chemical Research*, 2008, **41**, 157-167.
14. J. Xie, S. C. Kohale, W. L. Hase, S. G. Ard, J. J. Melko, N. S. Shuman and A. A. Viggiano, *The Journal of Physical Chemistry A*, 2013, **117**, 14019-14027.
15. J. Xie, J. Zhang and W. L. Hase, *International Journal of Mass Spectrometry*, 2015, **378**, 14-19.
16. J. Xie, R. Otto, R. Wester and W. L. Hase, *The Journal of Chemical Physics*, 2015, **142**, 244308.
17. J. Baker and P. Pulay, *The Journal of Chemical Physics*, 2002, **117**, 1441-1449.
18. A. P. Bento, M. Solà and F. M. Bickelhaupt, *Journal of Computational Chemistry*, 2005, **26**, 1497-1504.
19. M. W. Chase, *J. Phys. Chem. Ref. Data, Monograph 9*, 1998.
20. D. R. Lide, *CRC Handbook of Chemistry and Physics, Internet Version 2005*, CRC Press, Boca Raton, FL, 2005.
21. B. R. a. D. H. Bross, Active Thermochemical Tables (ATcT) values based on ver. 1.122p of the Thermochemical Network, available at ATcT.anl.gov).
22. L. A. Curtiss, P. C. Redfern, K. Raghavachari, V. Rassolov and J. A. Pople, *The Journal of Chemical Physics*, 1999, **110**, 4703-4709.
23. E. P.J. Linstrom and W.G. Mallard, **NIST Chemistry WebBook, NIST Standard Reference Database Number 69**, National Institute of Standards and Technology, Gaithersburg MD, 20899, <https://doi.org/10.18434/T4D303> (retrieved July 22, 2021)).
24. G. Knizia, *J Chem Theory Comput*, 2013, **9**, 4834-4843.
25. G. Knizia and J. E. M. N. Klein, *Angewandte Chemie International Edition*, 2015, **54**, 5518-5522.